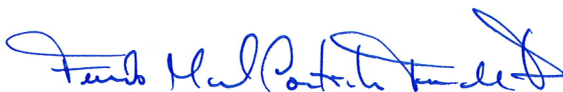## Classificação de Seminário PRODEM

O aluno do Programa Doutoral em Engenharia Mecânica (PRODEM) **Mohammadali Masoudian** apresentou a 20 de Dezembro de 2013, em sessão pública na Faculdade de Engenharia da Universidade do Porto, o Seminário de Elaboração do Projecto de Investigação do PRODEM, sob o título "Turbulence models for viscoelastic fluids", relativo aos trabalhos por si realizados até aquela data sob a orientação do Prof. Fernando Pinho, da FEUP.

Após discussão do trabalho apresentado pelo aluno o júri das provas atribuiu ao Seminário (correspondendo a 20 unidades de crédito ECTS) a classificação de 19 (dezanove) valores.

Porto, 20 de Junho de 2013

José M. A. César de Sá
(Professor Catedrático da FEUP, Director do PRODEM)

Fernando Manuel Coutinho Tavares de Pinho
(Professor Associado com Agregação da FEUP)

José Alexandre Costa da Silva Lopes
(Investigador Auxiliar da FEUP)

U.PORTO
FEUP FACULDADE DE ENGENHARIA
UNIVERSIDADE DO PORTO

Inscrição a título definitivo de doutorando PRODEM

O aluno do Programa Doutoral em Engenharia Mecânica (PRODEM) **Mohammadali Masoudian** apresentou a 20 de Dezembro de 2013, em sessão pública na Faculdade de Engenharia da Universidade do Porto, o Seminário de Elaboração do Projecto de Investigação do PRODEM, sob o título "Turbulence models for viscoelastic fluids", relativo aos trabalhos por si realizados até aquela data.

Tendo obtido no Seminário (correspondendo a 20 unidades de crédito ECTS) a classificação de 19 (dezanove) valores é agora dado parecer favorável à sua inscrição a título definitivo como doutorando PRODEM, sob a orientação do Prof. Fernando Manuel Coutinho Tavares de Pinho da FEUP.

Porto, 20 de Junho de 2013

José M. A. César de Sá
(Professor Catedrático, Director do PRODEM)

U.PORTO

FEUP FACULDADE DE ENGENHARIA
UNIVERSIDADE DO PORTO
Programa Doutoral em Engenharia Mecânica

Seminário de Elaboração do Projecto de Investigação

Turbulence models for viscoelastic fluids

Prepared by:

Mohammadali Masoudian

Supervised by:
Fernando Manuel Coutinho Tavares de Pinho
(Universidade do Porto - Faculdade de Engenharia / Departamento de
Engenharia Mecânica)

Acknowledgments

Abstract

Drag and heat transfer reductions (DR and HTR) by additives can be as high as 80% compared with Newtonian flows and are found in many industrial applications from long distance fluid transport to thermal fluids in district heating and cooling systems to oil and gas drilling and shipping. It has motivated extensive research and the wealth of data has allowed a comprehensive phenomenological description of DR in boundary layers , but modern engineering simulation tools are still unable to predict bulk turbulent flow characteristics from rheological properties. The understanding of the relationship between DR and fluid rheology has only started to unravel by Direct Numerical Simulations (DNS). Engineering computational tools depend on reliable turbulence models, which for non-Newtonian fluids are still in their infancy and are based exclusively on the Reynolds Average Navier-Stokes (RANS) methodology. Most existing non-Newtonian turbulence models are for inelastic fluids, unrelated to rheology or based on simplified viscoelastic rheology with no memory. Only very recent models [1-3] are based on true viscoelastic fluid models, such as the Finitely Extensible Non-Linear Elastic model –with Peterlin's approximation (FENE-P). The models should be checked against DNS data for low DR, up to maximum DR.

This thesis is aimed at further developing this area and this is achieved through various more specific objectives, namely the extension of existing RANS turbulence model to maximum DR, in particular the development of improved 1st and 2nd order closures for the Reynolds stresses, the development of the first ever turbulence model to predict heat transfer in turbulent flows of viscoelastic fluids, which involves the development of closures for the Reynolds scalar fluxes and finally the beginning of the development of a new family of turbulence models based on large eddy simulation (LES). In all cases the developments will be grounded on DNS data provided by research partners, even though it is not excluded that some reduced set of DNS can be obtained as part of this thesis.

Table of Contents

INTRODUCTION

Introduction

It has been known for quite sometime that the addition of polymers to turbulent flows of Newtonian fluids can dramatically reduce turbulent friction coefficient. It has been shown experimentally that very small amounts of polymers are sufficient to reduce drag up to 80%. Comprehensive reviews of the early literature in this area are given in Hoyt [4], Lumley [5,6] and Virk [7].

Several theories have been proposed to describe the complex mechanism of turbulent drag reduction (DR) with dilute polymer solutions. Lumley [5] proposed a mechanism based on the extension of the polymers, suggesting that the stretching of coiled polymers, in regions with strong deformations such as the buffer layer, increases the effective extensional viscosity. This would dampen small eddies, thicken the viscous sublayer and consequently lead to drag reduction. Lumley also related the onset of drag reduction with to the situation where the time scale of the polymers becomes larger than the time scale of the flow.

In his extensive experimental data analysis Virk [8] introduced the concept of an "elastic sublayer" existing between the viscous sublayer and the logarithmic zone and he suggested that this layer plays a crucial role in drag reduction. Virk [7] observed an increase in the thickness of this layer with drag reduction to eventually fill the whole logarithmic region at maximum drag reduction, thus introducing the concept of maximum drag reduction asymptote. De Gennes[9] postulated that drag reduction is caused by the elastic rather than the viscous properties of polymer additives. This idea is supported by experiments showing that drag reduction also occurs when the polymers are injected at the centre of the pipe (e.g. McComb & Rabie 1979, 1982), but these authors nevertheless concluded that in this case drag reduction was still a wall effect localized in the buffer layer. De Gennes' explanation is that the shear waves, which are caused by the elasticity of the polymers prevent production of turbulent velocity fluctuations at the small scales. Others [10-12] proposed different theories on the mechanisms of DR.

Over the last 15 years, the development of accurate and efficient numerical and experimental methods have made it possible to investigate in detail turbulent drag reduction in dilute polymer solutions [13-16]. It is now generally accepted that DR is associated with increased fluid resistance due to the high extensional viscosity of the viscoelastic polymer solutions leading to a reduction in the vortex dynamic activities that are characteristic of

turbulence. The crucial events take place near the wall, in the viscous and buffer sublayers, where the molecules become more extended. This is essentially in agreement with the original proposals of Metzner and Lumley [5,10].

A wealth of DNS investigations on fully-developed turbulent channel flow have been carried out since early this century aimed at shedding light on understanding different aspect of DR from the effect of polymer rheological parameters to the mechanisms of drag reduction [17-18]. These numerical simulations use constitutive equations based on the dumbbell where the two beads are usually connected by a nonlinear elastic spring, cf. Bird et al. 1987 [19]. The polymer dynamics is then entirely described by the evolution of the end-to-end vector connecting the two beads, represented as the phase-averaged configuration tensor. In a flow field, the evolution of the end-to-end vector is governed by the stretching and restoring forces acting on the dumbbell. The polymer model most often implemented for the study of DR is the FENE-P model [19] (FENE-P stands for finitely extensible nonlinear elastic model with Peterlin's approximation). Although there are competing models (e.g., FENE, Oldroyd-B, PTT), the FENE-P model is preferred because of its physical background for dilute polymer solutions, its accounting of finite extensibility of the molecule and simplicity (it uses a simple second-order closure model in the equation for the polymer stress tensor). Aside from being physically consistent with real polymers, finite extensibility reduces numerical instabilities, whereas the model simplicity reduces computational costs. Although the single dumbbell FENE-P model can capture the basic rheological properties of polymer solutions in many types of flows, there are clear circumstances in which the model does not capture the correct physics (Somasi et al. 2002). DNS simulation of turbulent viscoelastic flow is extremely expensive, significantly more expensive than Newtonian DNS, because of the larger number of primary variables in the former than in the latter. Additionally, as DR increases, the near wall streaks become progressively stabilized and elongated, thus requiring the use of longer simulation boxes in particular for high DR values [20]. Consequently, for a given Reynolds number, the CPU-time and memory requirements for the DNS of viscoelastic flows are at least one order of magnitude larger as compared to the Newtonian case, and it is not feasible for most of the engineering purposes Hence, Reynolds-averaged Navier–Stokes (RANS) type or other

numerically inexpensive models have to be developed for modeling turbulent flows of dilute polymer solutions.

The earlier attempts to develop turbulence closures for non- Newtonian fluids started by modifying the von Kármán coefficient in order to calculate drag reduction. Subsequent turbulence models included only variable viscosity effects, described by such rheological constitutive equations as the power law or Bingham law for yield stress fluids [21,22]. In an attempt to incorporate viscoelastic fluid rheology into turbulence models for drag reducing fluids, Pinho et.al. [23,24] developed several first-order turbulence models for a modified version of the generalised Newtonian fluid constitutive equation, where the dependence of strain hardening of the fluid on the third invariant of the rate of deformation tensor was included. This family of models also included an anisotropic version to capture the increased Reynolds stress anisotropy [24].

Leighton et al. [25] proposed the first turbulence model for polymer flows based on the FENE-P dumbbell constitutive equation model. In their closure, transport equations for the Reynolds and the polymer stresses were added to the mean flow equation and closures for the unknown correlations were developed and the model tested in channel flow, but the model was not made available in the open literature. Pinho et al. [1] devised a new RANS model for FENE-P fluids, which is an extension of the low Reynolds number k-ε closure for Newtonian fluids. This model provided closures for various terms of the governing equations, but only worked for low DR. Subsequently, Resende et al. [2] developed several sophisticated and complex closures for the nonlinear turbulent term of the conformation tensor equation and improved previous closures of Pinho et al. [1] for the viscoelastic stress work and the viscoelastic turbulent transport of the turbulent kinetic energy (k) extending the model to intermediate levels of drag reduction and showing the limitations of a simple k-ε approach to modeling. In fact, since turbulence anisotropy increases with DR, the inherent turbulence isotropy of k-ε leads to some conflicting variations. Hence, and even though their predictions are good for low and intermediate DR, their model cannot predict high DR and it has an excessive number of damping functions and coefficients, which makes it unattractive.

A contemporary model was that of Iaccarino et al. [3], who introduced a k-ε -v^2-f model for fully developed channel flow which is capable of predictions over the whole range of DR.

It is a fairly simple model, introducing the concept of turbulent polymer viscosity to account for the effects of polymers in the momentum equation that depends on the turbulent kinetic energy, the polymer relaxation time and the trace of constitutive equation. The model of the nonlinear terms in the conformation tensor equation relied on the turbulent dissipation rate, but the main characteristic of Iaccarino et al. model [3], imported from the corresponding Newtonian model, was the ability to input into the Reynolds stress tensor closure the effect of wall normal turbulence via the scalar v^2 and the role of pressure strain, quantities that are significantly modified by polymer additives which enhanced turbulence anisotropy. However, although their model predicts accurately the amount of drag reduction, in our opinion their predictions of polymer shear stress in the Reynolds-averaged momentum, turbulent kinetic energy and evolution equation for the conformation tensor are not in agreement with DNS results. In this work we aim to address these shortcomings by presenting two models of turbulence for FENE-P fluids, with closures at different level, i.e., one being a four model equation still invoking a Boussinescq hypothesis, the other developing closures for the full Reynolds stress tensor. We also aim to develop the first ever RANS type of model for the Reynolds calar fluxes, and finally we aim to start developing a new class of models based on the concept of large eddy simulation.

VISCOELASTIC CONSTITUTIVE EQUATIONS

1-1 Basic principles

Constitutive equations are relations that describe the complex rheological behavior of materials relating the stress tensor with the kinematic quantities. Depending on the mathematical relationship, the equation can be linear, quasi-linear or non-linear, but mostly are non-linear. This classification applies to viscoelastic fluids and the linear rheological constitutive equation is based on a simple principle where the response at any time is directly proportional to the value of the input signal, i.e., for example, for a fixed stress we obtain a directly proportional strain rate. The differential equations, in the linear viscoelasticity theory, are linear and the coefficients of the time differentials are defined by the material parameters. These material parameters such as, for example, the viscosity coefficient and the rigidity modulus, are constant not depending on variables such as strain or strain rate. The simplest constitutive equation used for viscoelastic fluids is based on the generalized Newtonian fluids constitutive equation, in these kind of models the viscosity is not constant and depends on the shear rate, capturing only the shear thinning/thickening effect of the polymeric solutions. This type of model is not viscoelastic because it is not able to predict the elastic contribution, i.e., it neither has memory effect nor normal stress effects [26]. A more severe limitation of the linear constitutive models is that they do not obey the principle of Oldroyd's material objectivity where they had to be formulated for general validity. The quasi-linear constitutive models solved this problem by replacing the material derivates with Oldroyd's convected derivates. For example, both the Upper Convected Maxwell (UCM) and the Oldroyd-B models result from a substitution of the material derivatives by the

contravariant convected derivate, and have the capacity to predict the first normal stress coefficient and are invariant to coordinate system changes.

The quasi-linear models are capable of describing time-dependent flows, however, these models are not able to portray well the rheological properties of the polymeric solutions. For example, the deficiencies of constant viscosity and normal stress coefficients in steady shear flow and the infinitive elongational viscosity at finite elongation rates.

1-2 FENE-P Model

In studying dilute polymeric solutions, the polymer molecules are often modeled as dumbbells consisting of two beads connected by a spring. In a flowing Newtonian solvent the dumbbells are convected and distorted by the viscous force exerted on the beads by the solvent. In the simplest model, the elastic force between the beads is taken to be proportional to the separation between the beads. This is the so-called Hookean dumbbell model. In addition to the forces mentioned above, the beads experience a randomly fluctuating force due to the thermal agitation by the surrounding solvent molecules. It can be shown that the constitutive equation associated with the Hookean dumbbell model is identical to the macroscopic Oldroyd-B equation. Due to its simplicity the model has some serious drawbacks, the most important being the fact that the shear viscosity is constant and that the dumbbells can be stretched infinitely. In elongational flow for example, this leads to an unbounded value of the elongational viscosity at high strain rate. A way to overcome these problems is to replace the Hookean spring by a non-linear spring to limit the dumbbell extension to a maximum value. An important

example of such a non-linear spring is the finitely extensible non-linear elastic (FENE) spring introduced by Warner [27].

A major drawback of the FENE model is that it does not yield a closed-form constitutive equation for the polymer stress. For this reason it is not suited for a macroscopic flow calculation. However, if expression for the connector force is replaced by its ensemble averaged value, it is possible to close the model. This pre-averaging is known as the Peterlin approximation and the resulting model as the FENE-P model.

The issue of whether a FENE-P is an adequate representation of the FENE model in the context of turbulent flow, and in particular turbulent channel flow, as also been investigated by Zhou and Akhavan [28], who concluded that the FENE-P dumbbell was accurate only in the steady state, incurring large errors at all phases of transient elongational flows. Contrasting to the FENE model demonstrated a good approximation in transient elongational flows. So, it is clear that an important step is the correct choice of the constitutive equation and as demonstrated they can be more or less complex, capturing more or less rheological properties. Sometimes a complex model is not the best choice, for example in channel turbulent flow without hysteretic behaviour, both FENE-P and FENE-LS models predict with the same accuracy, but the numerical complexity of the FENE-LS model increase significantly, and so the FENE-P model should be preferred instead of the FENE-LS model, at least at this initial stage of turbulence modelling of viscoelastic fluids. Note that the non-linear viscoelastic models do not resume the models described before. It is worth mentioning that besides the FENE-P models merits, there is some inaccurate predictions in direct numerical simulation of the channel flow, for example, in the experiments of Ptasinski et al. [15] the stream wise turbulence (u'^2) increases slightly by increasing DR

with a peak of u_{rms} reaching around 3.2 corresponding to a peak for k of around 5.5. On the other hand their corresponding DNS results over-predict those peak values (maximum urms of around 4.5, and maximum k of around 8.5). They extensively discuss this difference and state that this might be due to shortcomings in the FENE-P model.

1-3 FENE-P Constitutive Equation

In this work the FENE-P model is used to calculate an extra stress due to the polymeric presence, and so the total stress is a combination of a solvent stress and polymeric stress, given by the following Eq. (1-1),

$$\tau_{ij} = \tau_{ij,s} + \tau_{ij,p} \tag{1-1}$$

$$\tau_{ij,s} = 2\eta_s S_{ij} \tag{1-2}$$

where the τ_s is solvent stress, S is the rate of deformation tensor and η_s is the constant shear viscosity of the solvent. The polymeric stress of the Eq. (1-1) (τ_p) is based on the FENE-P model and given by Eq. (1-3), but presented now in dimensionless form

$$\tau_{ij,p} = \frac{\eta_p}{\lambda} \left[f(C_{kk}) C_{ij} - f(L) \delta_{ij} \right] \tag{1-3}$$

where η_p is the polymeric viscosity coefficient and C_{ij} is the conformation tensor which is determined by an evolution equation using Oldroyd's upper convective derivate of C_{ij} to keep the material objectivity, i.e.

$$\left(\frac{\partial C_{ij}}{\partial t} + \hat{U}_k \frac{\partial C_{ij}}{\partial t} - C_{jk} \frac{\partial U_i}{\partial x_k} - C_{ik} \frac{\partial U_j}{\partial x_k} \right) = -\frac{\tau_{ij,p}}{\eta_p} \tag{1-4}$$

The functions appearing in the polymer stress are

$$f(C_{kk}) = \frac{L^2 - 3}{L^2 - C_{kk}}$$

(1-5)

and

$$f(L) = 1$$

where L^2 is the maximum extensibility of the dumbbell model.

Reynolds-averaging the above equations, the time-averaged polymer stress $\overline{\tau}_{ij,p}$ is now given by:

$$\overline{\tau}_{ij,p} = \frac{\eta_p}{\lambda}\left[f(C_{kk})C_{ij} - f(L)\delta_{ij}\right] + \frac{\eta_p}{\lambda}\overline{f(C_{kk} + c_{kk})c_{ij}}$$

(1-6)

where the last term on the right hand side also needs an approximation.

The time-averaged form of the conformation tensor evolution equation is:

$$\overset{\triangledown}{C}_{ij} + \overline{u_k \frac{\partial c_{ij}}{\partial x_k}} - \left(\overline{c_{jk}\frac{\partial u_i}{\partial x_k}} + \overline{c_{ik}\frac{\partial u_j}{\partial x_k}}\right) = -\frac{\overline{\tau}_{ij,p}}{\eta_p}$$

(1-7)

which after substitution of eq. (6), becomes:

$$\lambda \overset{\triangledown}{C}_{ij} + \lambda\left(\overline{u_k \frac{\partial c_{ij}}{\partial x_k}} - \left(\overline{c_{jk}\frac{\partial u_i}{\partial x_k}} + \overline{c_{ik}\frac{\partial u_j}{\partial x_k}}\right)\right) = -\left[f(C_{kk})C_{ij} - f(L)\delta_{ij} + \overline{f(C_{kk} + c_{kk})c_{ij}}\right]$$

(1-8)

On the left hand side of Eqs. (8) the mean flow advective term contained within the Oldroyd derivative of C_{ij} ($\overset{\triangledown}{C}_{ij}$) is null for fully developed channel flow. The mean flow distortion term of $\overset{\triangledown}{C}_{ij}$ by the mean flow is M_{ij} and is given by:

16

$$M_{ij} = \left(C_{jk} \frac{\partial U_i}{\partial x_k} + C_{ik} \frac{\partial U_j}{\partial x_k} \right) \tag{1-9}$$

M_{ij} is finite, but is exact therefore its needs no closure. The remaining two terms are related to turbulence and following the analysis and nomenclature of Li et al. [20] they are labeled as

$$CT_{ij} = -\overline{u_k \frac{\partial c_{ij}}{\partial x_k}} \tag{1-10}$$

which represents the contribution to the advective transport of the conformation tensor by the fluctuating velocity field, and

$$NLT_{ij} = \overline{c_{jk} \frac{\partial u_i}{\partial x_k}} + \overline{c_{ik} \frac{\partial u_j}{\partial x_k}} \tag{1-11}$$

which accounts for the interactions between the fluctuating components of the conformation tensor and of the velocity gradient tensor. This term originates from the Oldroyd derivative and is the fluctuating counterpart of M_{ij}. Both CT_{ij} and NLT_{ij} require closure approximations.

TURBULENCE

Turbulence

2-1. Introduction

Many of the flows we encounter in daily life are turbulent. Typical examples are flow around (as well as *in*) cars, airplanes and buildings. The boundary layers and the wakes around and after bluff bodies such as cars, airplanes and buildings are turbulent. Also the flow and combustion in engines, both in piston engines and gas turbines and combustors, are highly turbulent. Air movements in rooms are turbulent, at least along the walls where wall-jets are formed. Hence, when we compute fluid flow it will most likely be turbulent. There is no definition on turbulent flow, but it has a number of characteristic features (see Pope [29] and Tennekes & Lumley [30]) such as:

I. *Irregularity*. Turbulent flow is irregular, random and chaotic. The flow consists of a spectrum of different scales (eddy sizes). We do not have any exact definition of *turbulent eddy*, but we suppose that it exists in a certain region in space for a certain time and that it is subsequently destroyed (by the cascade process or by dissipation). It has a characteristic velocity and length (called velocity and length scales). The region covered by a large eddy may well enclose also smaller eddies. The largest eddies are of the order of the flow geometry (i.e. boundary layer thickness, jet width, etc). At the other end of the spectra we have the smallest eddies which are dissipated by viscous forces (stresses) into thermal energy resulting in a temperature increase. Even though turbulence is chaotic it is deterministic and is described by the Navier-Stokes equations for Newtonian fluids.

II. Diffusivity. In turbulent flow the diffusivity increases. The turbulence increases the exchange of momentum in e.g. boundary layers, and reduces or delays thereby separation at bluff bodies such as cylinders, airfoils and cars. The increased diffusivity also increases the resistance to motion (wall friction) and heat transfer in internal flows such as in channels and pipes.

III. Large Reynolds Numbers. Turbulent flow occurs at high Reynolds number. For example, the transition to turbulent flow in pipes occurs at $Re_D = 2300$ and in boundary layers at $Re_x \sim 500{,}000$.

IV. Three-Dimensional. Turbulent flow is always three-dimensional and unsteady. However, when the equations are time averaged, we can treat the flow as two-dimensional or even one-dimensional.

V. Dissipation. Turbulent flow is dissipative, which means that kinetic energy in the small (dissipative) eddies are transformed into thermal energy. The small eddies receive the kinetic energy from slightly larger eddies. The slightly larger eddies receive their energy from even larger eddies and so on. The largest eddies extract their energy from the mean flow. This process of transferring energy from the largest turbulent scales (eddies) to the smallest is called the cascade process.

VI. Continuum. Even though we have small turbulent scales in the flow they are much larger than the molecular scale and we can treat the flow as a continuum.

2-2. Governing Equations

In this section time- averaged equations are presented. In what follows, upper-case letters or overbars denote time-averaged quantities and lower-case letters or primes denote fluctuating quantities. A hat denotes an instantaneous quantity.

Continuity and momentum equations

The time-averaged equations appropriate for incompressible FENE-P fluid are:

Continuity:

$$\frac{\partial U_i}{\partial x_i} = 0 \qquad (2\text{-}1)$$

Momentum:

$$\rho \frac{\partial U_i}{\partial t} + \rho U_k \frac{\partial U_i}{\partial x_k} = -\frac{\partial \overline{P}}{\partial x_i} - \frac{\partial}{\partial x_k}(\overline{\rho u'_i u'_k}) + \frac{\partial \overline{\tau}_{ik}}{\partial x_k} \qquad (2\text{-}2)$$

where $\overline{\tau}_{ik}$ is the time-averaged total extra stress tensor, U_i is the mean velocity, $\overline{P}$ is the mean pressure, ρ is the fluid density and $\overline{\rho u_i u_k}$ is the Reynolds stress tensor. The extra stress tensor $\overline{\tau}_{ij}$ in eq. (2-2) describes the rheology of the fluid and is given in eq. (2-3) as the sum of a Newtonian solvent contribution of viscosity η_S with a polymeric contribution $\overline{\tau}_{ij,p}$ described by the FENE-P rheological constitutive model.

$$\overline{\tau}_{ij} = 2\eta_s \overline{S}_{ij} + \overline{\tau}_{ij,p} \tag{2-3}$$

S_{ij} is the rate of strain tensor defined as

$$S_{ij} = \frac{1}{2}\left(\frac{\partial U_i}{\partial x_j} + \frac{\partial U_j}{\partial x_i}\right) \tag{2-4}$$

In eqs. (2-2) and (2-3) the Reynolds stress and time-averaged polymer stress need approximations. Regarding the former, it can be calculated by models developed for Newtonian fluids but modified to account for the effects of viscoelasticity, whereas the latter must be calculated with the rheological constitutive equation.

The Exact $\overline{u'_i u'_k}$ Transport Equation

The most comprehensive Reynolds averaged turbulence model is based on the exact transport equations for the turbulent stresses. An exact equation for the Reynolds stresses can be derived from the Navies-Stokes equation. It is emphasized that this equation is exact; or, rather, as exact as the Navier-Stokes equations. The derivation follows the steps below. More details can also be found in [29-31]

$$\frac{\partial \overline{u'_i u'_j}}{\partial t} + U_k \frac{\partial \overline{u'_i u'_j}}{\partial x_k} = \tag{2-5}$$

$$\underbrace{\left(-\overline{u'_i u'_k}\frac{\partial U_j}{\partial x_k} - \overline{u'_j u'_k}\frac{\partial U_i}{\partial x_k}\right)}_{P_{ij}} + \underbrace{\frac{\partial}{\partial x_k}\left(\nu \frac{\partial \overline{u'_i u'_j}}{\partial x_k}\right)}_{D_{ij,\nu}} - \underbrace{\frac{\partial}{\partial x_k}\left(\overline{u'_i u'_j u'_k} + \frac{\overline{p'}}{\rho}\left(\delta_{jk}u'_i + \delta_{ik}u'_j\right)\right)}_{D_{ij,t}}$$

$$\underbrace{-2\nu\overline{\frac{\partial u'_i}{\partial x_k}\frac{\partial u'_j}{\partial x_k}}}_{\varepsilon_{ij}} + \underbrace{\frac{\overline{p'}}{\rho}\left(\frac{\partial u'_i}{\partial x_j} + \frac{\partial u'_j}{\partial x_i}\right)}_{\Pi_{ij}} + \underbrace{\frac{\partial}{\partial x_k}\left(\overline{u'_i \tau_{jk,p}} + \overline{u'_j \tau_{ik,p}}\right)}_{D_{ij,p}} - \underbrace{\left(\overline{\tau_{ik,p}\frac{\partial u'_j}{\partial x_k}} + \overline{\tau_{jk,p}\frac{\partial u'_i}{\partial x_k}}\right)}_{\varepsilon_{ij,p}}$$

22

Except for the last two terms on the right hand side, the other terms are classical terms appearing in Newtonian fluid models and represent the turbulence production by the mean strain (P_{ij}), molecular diffusion ($D_{ij,v}$), turbulent transport ($D_{ij,t}$), viscous dissipation by the solvent (ε_{ij}) and the pressure–strain term ($\Pi_{ij,v}$). The last two terms are viscoelastic terms represent the viscoelastic turbulent transport ($D_{ij,p}$) and the viscoelastic stress work ($\varepsilon_{ij,p}$).

The Boussinesq assumption

In the Boussinesq assumption an eddy (i.e. a turbulent) viscosity is introduced to model the unknown Reynolds stresses in Eq. (2-2). The stresses are modeled as

$$\overline{u'_i u'_j} = -\nu_T \left(\frac{\partial \overline{u_i}}{\partial x_j} + \frac{\partial \overline{u_j}}{\partial x_i} \right) + \frac{2}{3}\delta_{ij}k = 2\nu_T \overline{S}_{ij} + \frac{2}{3}\delta_{ij}k \tag{2-6}$$

The last term is added to make the equation valid also when it is contracted (i.e taking the trace); after contraction both left and right side are equal (as they must be) and equal to $\overline{u'_i u'_i} = 2k$. When above equation is included in Eq. (2-2) we replace 6 turbulent stresses with one new unknown (the turbulent viscosity, ν_T). This is of course a drastic simplification.

It is important to recognize that the viscosity (ν) is physical parameters which depend on the fluid (e.g. water or air) and its conditions (e.g. temperature). However, the turbulent viscosity (ν_T), depends on the flow (e.g. mean flow gradients and turbulence).

The transport equation of k

The turbulent kinetic energy is the sum of all normal Reynolds stresses, i.e.

$$k = \frac{1}{2}\left(\overline{u_1'^2} + \overline{u_2'^2} + \overline{u_3'^2}\right) \equiv \frac{1}{2}\overline{u_i'u_i'} \tag{2-7}$$

By taking the trace (setting indices $i = j$) of the equation for $\overline{u_i'u_j'}$ and dividing by two we get the equation for the turbulent kinetic energy:

$$U_j \frac{\partial k}{\partial x_j} = P_k - \varepsilon + \frac{\partial}{\partial x_j}\left(\left(v + \frac{v_T}{\sigma_k}\right)\frac{\partial k}{\partial x_j}\right) - \left(\overline{\tau_{ij}^p \frac{\partial u_i}{\partial x_j}}\right) + \frac{\partial}{\partial x_j}\left(\overline{\tau_{ij}^p u_i}\right) \tag{2-8}$$

Except for the last two terms on the right hand side, the other terms are classical terms appearing in Newtonian fluid models and represent the advection of k, turbulence production by the mean strain ($P_k = 2v_t S_{ij}^2$), dissipation (ε), molecular diffusion and turbulent diffusion, and two viscoelastic terms respectively. The two viscoelastic terms require closure and represent the viscoelastic turbulent transport ($Q_p \equiv \partial\left(\overline{\tau_{ij}^p u_i}\right)/\partial x_j$) and the viscoelastic stress work ($\varepsilon_p \equiv \overline{\tau_{ij}^p \partial u_i/\partial x_j}$).

The transport equation of ε (rate of dissipation by the solvent)

Two quantities are usually used in eddy-viscosity model to express the turbulent viscosity, k and ε, in previous section we introduced the transport equation of the k for FENE-P fluids. The transport equation of ε based on [29] for viscoelastic fluid can be written as

$$\frac{\partial \varepsilon}{\partial t} + \overline{u_j}\frac{\partial \varepsilon}{\partial x_j} = \frac{\varepsilon}{k}\left(c_{\varepsilon 1}P^\varepsilon - c_{\varepsilon 2}\varepsilon\right) + \frac{\partial}{\partial x_j}\left[\left(v + \frac{v_t}{\sigma_\varepsilon}\right)\frac{\partial \varepsilon}{\partial x_j}\right] - E_p \tag{2-9}$$

Here, all terms are conceptually identical to those for a Newtonian fluid except for the last term (E_p) representing the viscoelastic contribution to the transport equation of ε. The definition and exact form of E_p were derived by Pinho et al. [1-2] and is given by:

$$E_p = 2\nu_s \frac{\eta_p}{\lambda\left(L^2 - 3\right)} \overline{\frac{\partial u_i}{\partial x_m} \frac{\partial}{\partial x_k} \left\{ \frac{\partial}{\partial x_m} \left[f\left(C_{mm}\right) f\left(\hat{c}_{pp}\right) c'_{qq} C_{ik} \right] \right\}}$$

(2-10)

A k-ε-$\overline{v^2}$-f MODEL FOR FENE-P FLUIDS

During the first year, a tensorially consistent near-wall four equation model is developed to model turbulent flow of dilute polymer solutions. The model is validated up to the maximum drag reduction limit, by utilizing the data obtained from direct numerical simulations using the Finitely Extensible Nonlinear Elastic-Peterlin (FENE-P) constitutive model. Eight sets of direct numerical simulation (DNS) data are used to analyze budgets of relevant physical quantities, such as the nonlinear terms in the FENE-P constitutive equation, the turbulent kinetic energy, the wall normal Reynolds stress and dissipation transport. Closures were developed in the framework of the k-ε-$\overline{v^2}$ - f model for the viscoelastic stress work, the viscoelastic destruction of the rate of dissipation, the viscoelastic turbulent viscosity, and the interactions between the fluctuating components of the conformation tensor and of the velocity gradient tensor terms. Predicted polymer stress, velocity profiles and turbulent flow characteristics are all in good agreement with the literature, and independent DNS data over a wide range of rheological and flow parameters, and show significant improvements over the corresponding predictions of other existing models. The published paper is presented in appendix A.

A REYNOLDS STRESS MODEL FOR FENE-P FLUIDS

(Ongoing work)

According to the time averaged governing equations presented in the first and second chapters the unknown terms which require closures in the time averaged FENE-P constitutive equation are:

1) Second term on the right-hand-side of Eq. 12 : $\overline{f(C_{kk}+c'_{kk})c'_{ij}}$

2) First term on the left-hand-side of Eq. 14, CT_{ij}: $\overline{-u'_k \dfrac{\partial c'_{ij}}{\partial x_k}}$

3) Second term on the left-hand-side of Eq. 14, NLT_{ij}: $\overline{c'_{jk}\dfrac{\partial u'_i}{\partial x_k}} + \overline{c'_{ik}\dfrac{\partial u'_j}{\partial x_k}}$

and unknown terms appearing in the Reynolds stress transport equation can be summarize as:

1) viscoelastic turbulent transport $D_{ij,p}$

2) the viscoelastic stress work $\varepsilon_{ij,p}$

Finally, the only term which requires closure in the dissipation transport equation is the viscoelastic contribution to the dissipation transport equation (E_p).

Fifteen sets of DNS results were used to quantify the budgets of these unknown terms, Moreover the DNS data are used to capture the influence of the rheological (Wi , L^2), and flow (Re) parameters in order to devise a powerful model. The work is not finished yet, however some predictions can be summarized as follows.
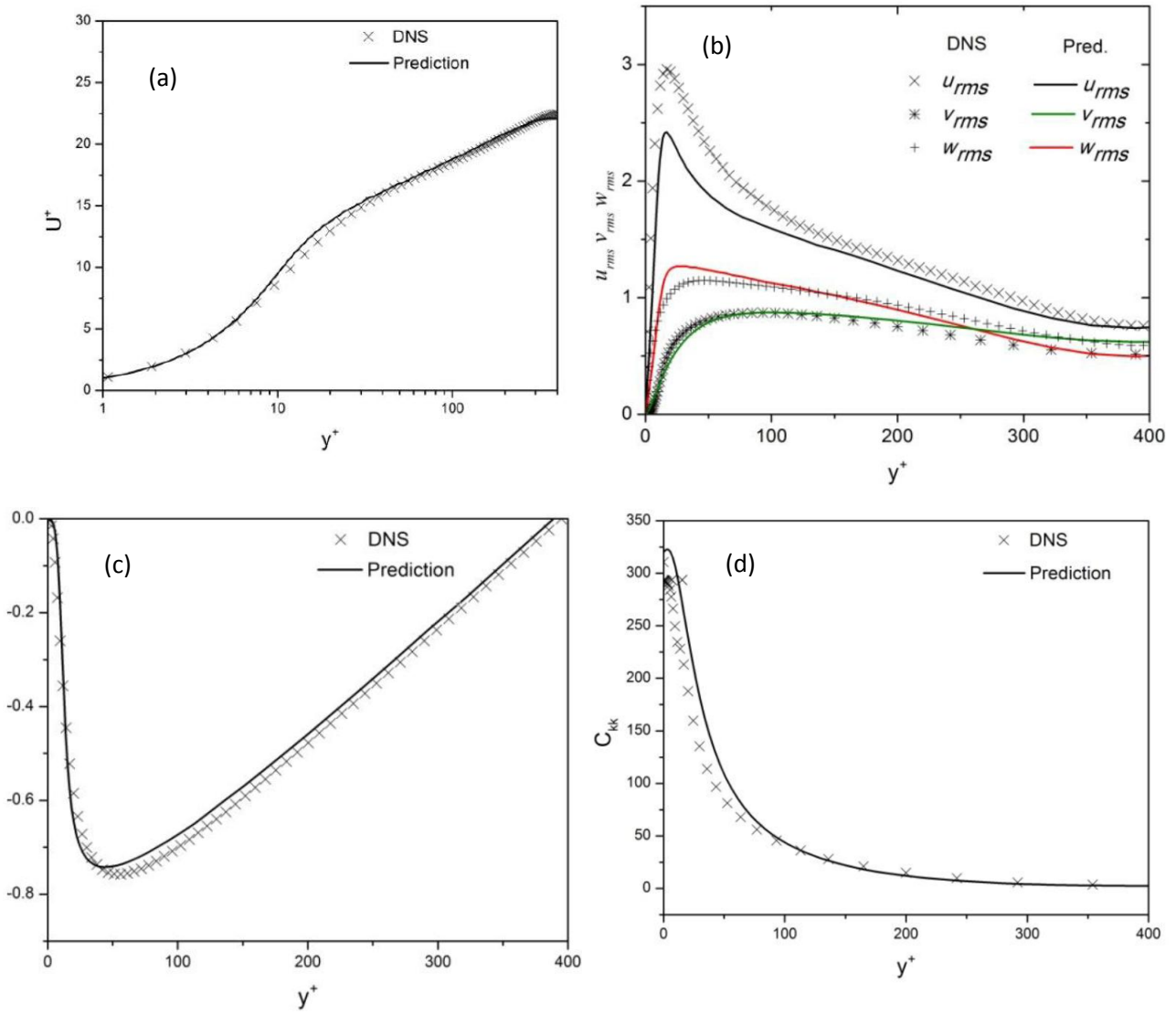
Fig. (4-1) Predictions of RSM closure a) mean velocity b) $u_{rms}, v_{rms}, w_{rms}$ c) shear Reynolds stress d) polymer length rheological parameters: $Wi=50$, $L^2=900$ at $Re_w=395$

GRID AND SUBGRID SCALE INTERACTIONS IN
VISCOELASTIC TURBULENT CHANNEL FLOW BY THE
AID OF DIRECT NUMERICAL SIMULATION
(Ongoing work)

The concept of energy cascade was introduced by Richardson in 1922 and briefly the idea is that kinetic energy of turbulence enters the turbulence (through the production mechanism) at the largest scales of motion, it is then transferred (by inviscid processes) to smaller and smaller scales until, at smallest scales, the energy is dissipated by viscous action. With the presence of polymers, the energy cascade is different from the one described earlier. As it was already mentioned, and based on Cai et al. [32], Casciola and De Angelis [33], polymers absorb turbulent kinetic energy from large and intermediate scales flow structures to feed the micro-structure at a different scale and dissipate it by elasticity and at small scales the energy is transferred from polymer micro-structures to the small-scale flow structures. The main goal of this section is to understand the routes of the turbulent kinetic energy, i.e. the interaction between grid scale (GS) and subgrid scale (SGS), between SGS and the polymer kinetic energy. For this reasons different kinds of filters are applied on instantaneous DNS data to identify the appropriate filter size for viscoelastic turbulent channel flow. The appropriate transport equations for the GS and SGS kinetic energy were derived for viscoelastic FENE-P fluids and the budgets of different terms were analyzed. In figures (5-1), (5-2) instantaneous DNS statistics are used to identify different terms in GS/SGS kinetic energy transport equations and different filter sizes are used to filter these quantities. Note that here only results of the box filter only are being presented.

The transport equation for the GS kinetic energy (the $\langle\ \rangle$ denotes filtering operator), is:

$$\underbrace{\frac{\partial\langle u_i\rangle.\langle u_i\rangle}{\partial t}}_{(1)}+\underbrace{\frac{\partial\langle u_i\rangle.\langle u_i\rangle.\langle u_j\rangle}{\partial x_j}}_{(2)}=-\underbrace{\frac{2}{\rho}\frac{\partial\langle p\rangle.\langle u\rangle_i}{\partial x_i}}_{(3)}+\underbrace{\frac{1}{\text{Re}_\tau}\frac{\partial}{\partial x_j}\left(\frac{\partial\langle u_i\rangle.\langle u_i\rangle}{\partial x_j}\right)}_{(4)}-\underbrace{\frac{2}{\text{Re}_\tau}\frac{\partial\langle u_i\rangle}{\partial x_j}\frac{\partial\langle u_i\rangle}{\partial x_j}}_{(5)}- \qquad (5\text{-}1)$$

$$\underbrace{2\frac{\partial\tau_{ij}\langle u_i\rangle}{\partial x_j}}_{(6)}+\underbrace{2\tau_{ij}\langle S_{ij}\rangle}_{(7)}+\underbrace{2\frac{\partial\langle T_{p,ij}\rangle.\langle u_i\rangle}{\partial x_j}}_{(8)}\underbrace{-2\langle T_{p,ij}\rangle.\langle S_{ij}\rangle}_{(9)}$$

The transport equation for the SGS kinetic energy, is:

$$\underbrace{\frac{\partial\tau_{ii}}{\partial t}}_{(10)}+\underbrace{\frac{\partial\tau_{ii}.\langle u_j\rangle}{\partial x_j}}_{(11)}=\underbrace{\frac{\partial}{\partial x_j}\left(\langle u_iu_i\rangle.\langle u_j\rangle-\langle u_iu_iu_j\rangle\right)}_{(12)}-\underbrace{\frac{2}{\rho}\frac{\partial}{\partial x_i}\left(\langle p\rangle.\langle u_i\rangle-\langle pu_i\rangle\right)}_{(13)}+\underbrace{\frac{1}{\text{Re}_\tau}\frac{\partial}{\partial x_j}\left(\frac{\partial\tau_{ii}}{\partial x_j}\right)}_{(14)}- \qquad (5\text{-}2)$$

$$\underbrace{\frac{2}{\text{Re}_\tau}\left(\left\langle\frac{\partial u_i}{\partial x_j}\frac{\partial u_i}{\partial x_j}\right\rangle-\frac{\partial\langle u_i\rangle}{\partial x_j}\frac{\partial\langle u_i\rangle}{\partial x_j}\right)}_{(15)}+$$

$$\underbrace{2\frac{\partial\tau_{ij}\langle u_i\rangle}{\partial x_j}}_{(16)}+\underbrace{-2\tau_{ij}\langle S_{ij}\rangle}_{(17)}+\underbrace{2\frac{\partial\langle T_{p,ij}u_i\rangle}{\partial x_j}}_{(18)}-\underbrace{2\frac{\partial\langle T_{p,ij}\rangle.\langle u_i\rangle}{\partial x_j}}_{(19)}\underbrace{-2\langle T_{p,ij}S_{ij}\rangle}_{(20)}+\underbrace{2\langle T_{p,ij}\rangle.\langle S_{ij}\rangle}_{(21)}$$

For the following cases the flow and rheological parameters are: $Re_{wall}=395$, $Wi_{wall}=50$, $L^2=3600$, Grid: $128\times129\times64$
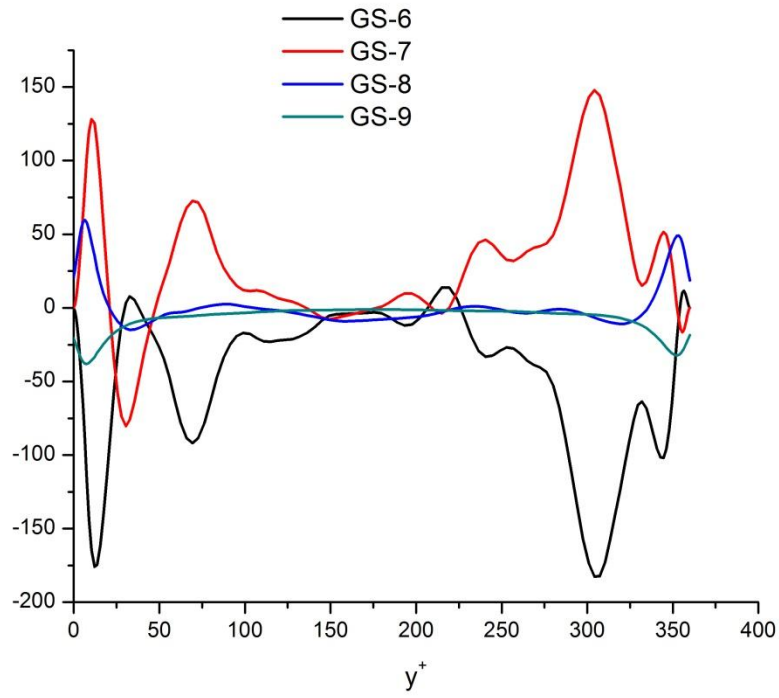
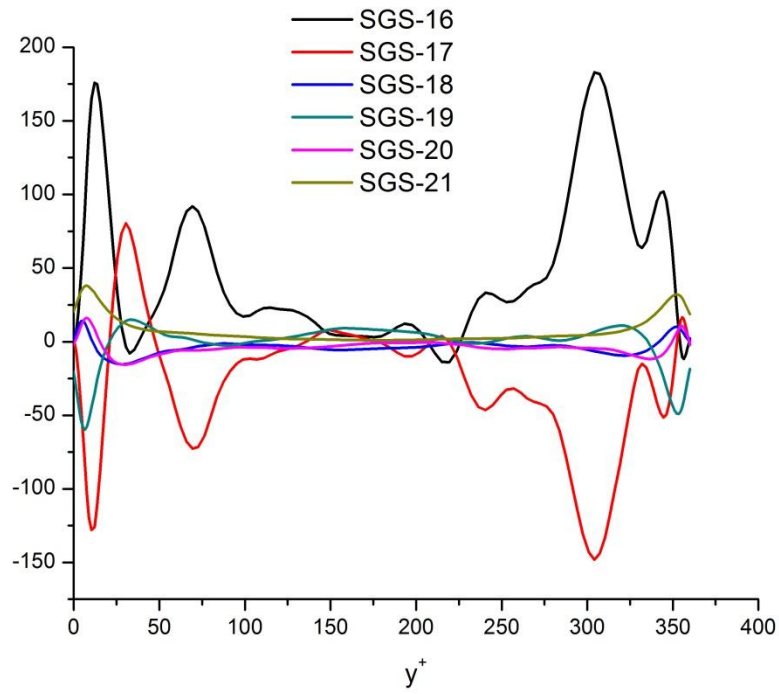Fig. (5-1) Last 4 terms in GS equation (spatial averaged)

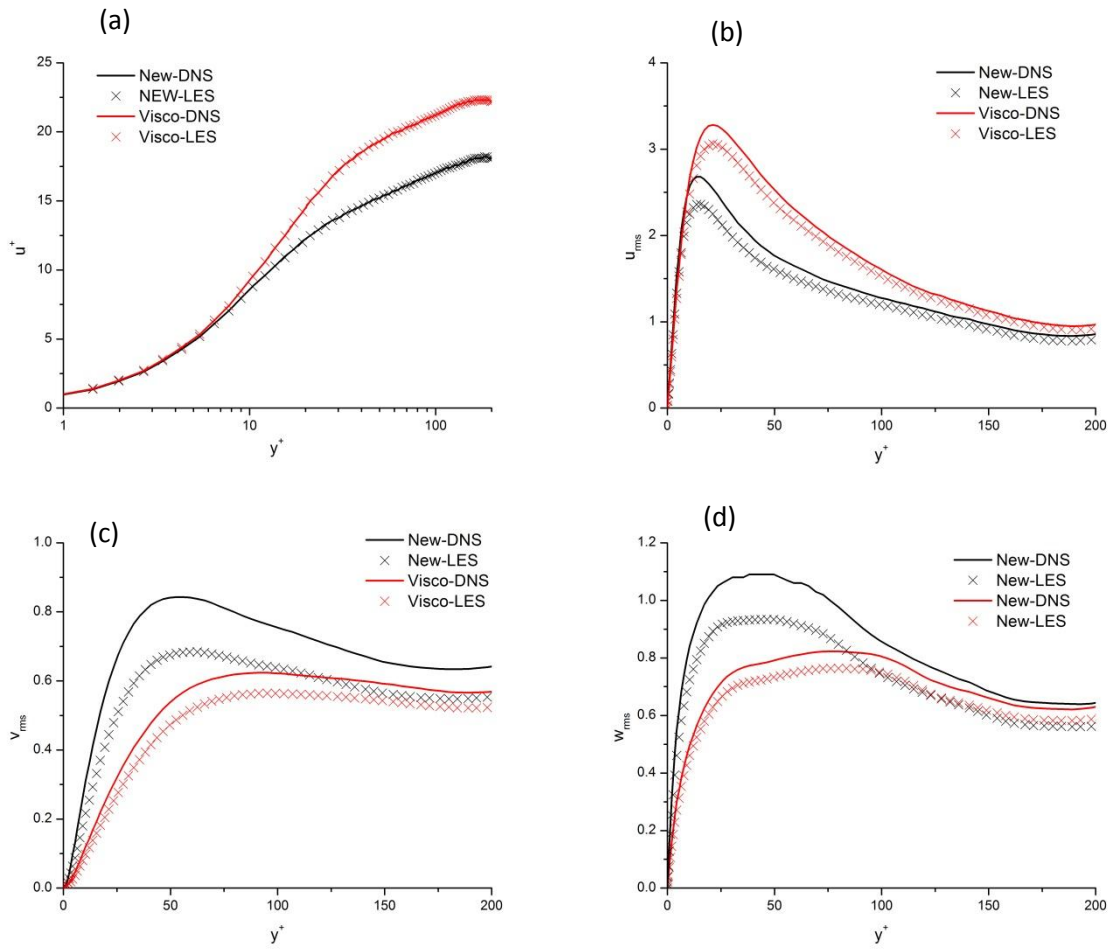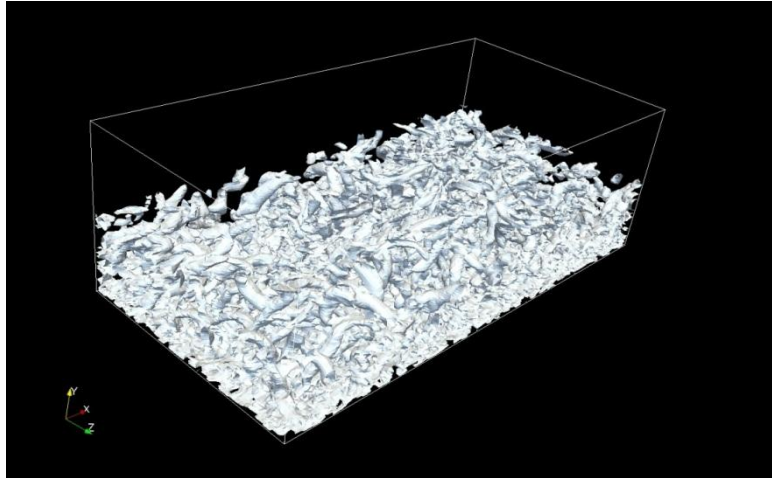
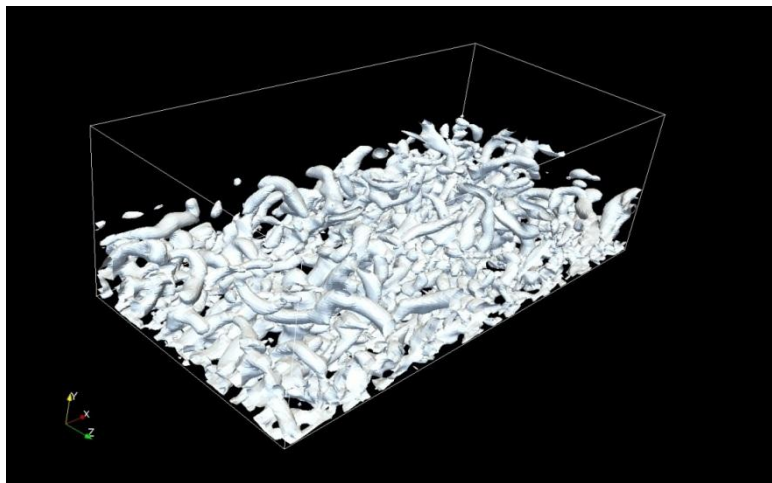Fig. (5-2) Last 6 terms in SGS equation (spatial averaged)

Fig. (5-3) Solid line: DNS, symbols: Box filter, a)Mean velocity profile, b) RMS of streamvise velocity fluctuation component, c) RMS of wall normal velocity fluctuation component, d) RMS of spanwise velocity fluctuation component (filter $\Delta/\Delta x=3$)

NEWTONIAN
DNS

NEWTONIAN
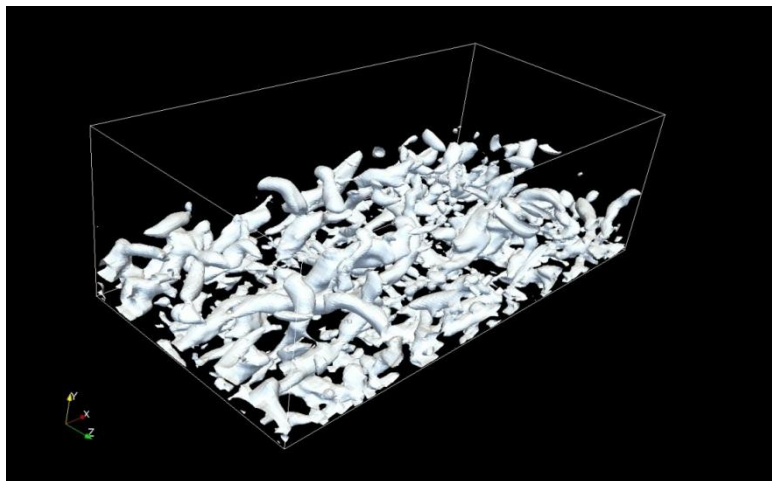with 4dx filter size

NEWTONIAN
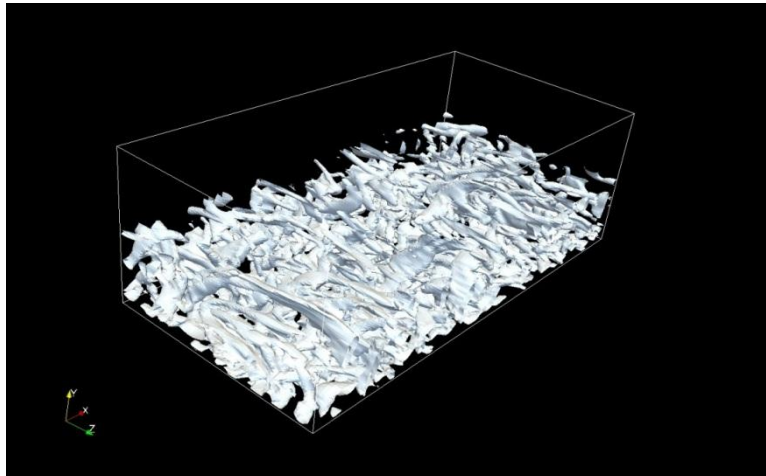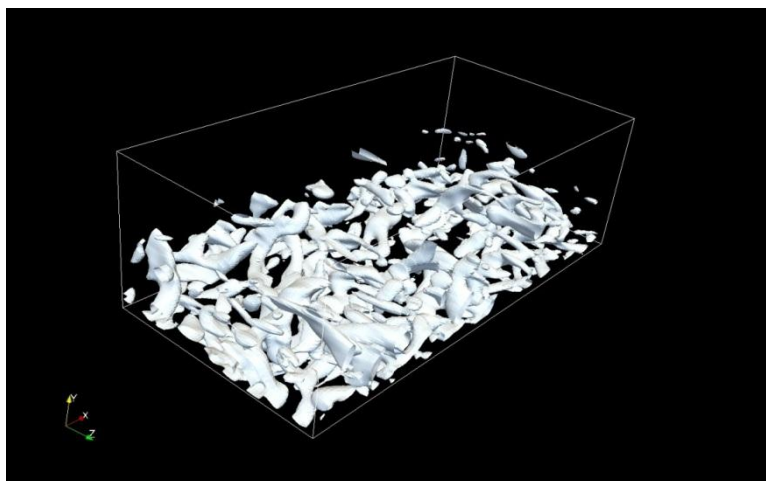with 6dx filter size

Fig. (5-4) Q-criteria visualization of Newtonian channel flow by
using different size of box filter

VISCOELASTIC
DNS

VISCOELASTIC
with 4dx filter size
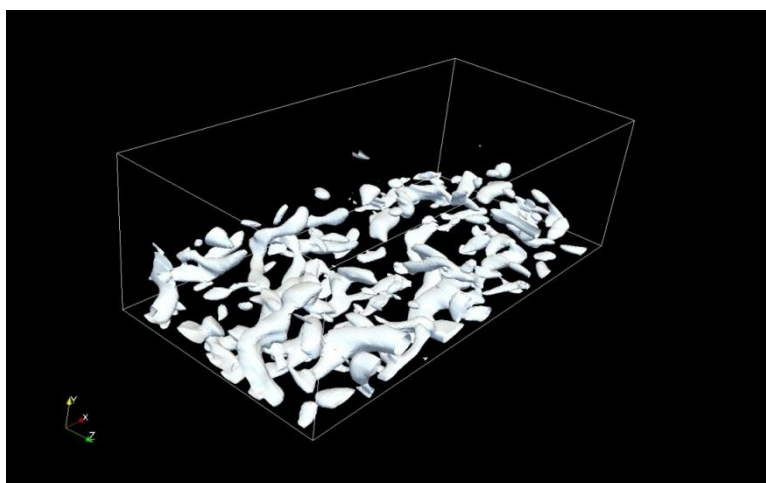

VISCOELASTIC
with 6dx filter size

Fig. (5-5) Q-criteria visualization of Viscoelastic channel flow by using
different size of box filter

WORK PLAN

Work Plan

The overall objective is the development of reliable turbulence closures for viscoelastic fluids, represented by the FENE-P viscoelastic constitutive equation. This will be accomplished via: Reynolds-Average Navier-Stokes/ Reynolds-Average Conformation Evolution (RANS/RACE) models. These approaches will be developed with a-priori and a-posteriori testing using adequate post-processing of existing Direct Numerical Simulation (DNS) data for fully developed channel flow.

The development of turbulence closures will be carried out via canonical flows for which the transport equation are simple. Therefore, for the RANS/RACE work we will not be using 3D codes, but specific 1D and 2D codes, which are small, effective and simple to program and run. This follows the method used by the host research group in previous work [1,2].

The candidate wishes to pursue the RANS/RACE turbulence model developments along the following lines:

1) The existing model is for low and intermediate levels of drag reduction and needs to be extended to the whole range of DR. This will be accomplished on the basis of a different base model, the k-epsilon-v^2-f model of Durbin [34]. A major feature of viscoelastic wall flows is the severe reduction of transverse normal Reynolds stress, and the k-epsilon-v^2-f model offers the possibility of an improved closure in the context of first order models.

Note that this part of the work has been accomplished to a large extent at the moment of writing this document and as documented in chapter 3.

2) Develop a low Reynolds number second order Reynolds stress model for FENE-P fluids for all regimes of DR. This involves the development of the

closures for NLT_{ij}, and the viscoelastic stress work for all components of Reynolds stress tensor, even though with more emphasis for their traces, as I have done for k-epsilon-v^2-f model above, So, the novelty here, in addition to adaptations of the closures for NLT_{ij}, and the viscoelastic stress work tensor, will be the modification of the pressure strain closure to include effects of viscoelasticity. These modifications will be essential to reduce the transfer of turbulent energy between Reynolds stress tensor components as the Weissenberg number and DR increases.

3) A Reynolds scalar flux model for FENE-P fluids will be developed also with the help of DNS data for fully-developed dynamic and thermal flow in a channel [35] and incorporated into the 1st and 2nd order turbulence models.

4) In collaboration with the partners of the project at IDMEC-IST I will start analyzing DNS data of flows of FENE-P fluids in turbulent channel flows, in order to assess the performance of the developed RANS/RACE closures so that at the end the turbulence models described above are able to predict both turbulent flows of FENE-P fluids near and away from walls.

5) The DNS results will be filtered in order to analyze energy cascade by analyzing the energy transfer between large and small flow scales in different zones of the energy spectrum. The separation between scales will be done using filtering operations in the physical space and the results will be analyzed using statistical tools. With the results obtained it will be possible to plan how to do LES of viscoelastic turbulent channel flows.

The above description involves a significant amount of work and by itself constitutes enough material for a PhD thesis. Nevertheless, there might also be the possibility to start developing a simple LES based turbulence model for FENE-P fluids in collaboration with the same team from IDMEC-IST. This requires new sets of DNS data with specific filtering still to be carried out.

Work Break Down		
Task	Stage	Deliverables
Literature review	(mandatory) Done	Internal Report
Finding the most stable and more relevant sort of Newtonian turbulent model	(mandatory) Done	Internal Report
Developing governing equations for viscoelastic turbulent flow	(mandatory) Done	Internal Report
k-epsilon-v^2-f	(mandatory) Done	Published (App. a)
Reynolds stress model (RSM)	Most of the Task is finished (mandatory)	(Internal review)
Performing DNS in FEUP	Done (Optional)	Internal Report
LES budgets and GS/SGS Interactions (Collaboration with C.Silva IST)	In the middle (Optional)	In Progress
RANS Scalar fluxes model for FENE-P fluids	0% (mandatory)	0%
DNS of the Jet flow or Elastic turbulence (haven't decided yet)	0% (Optional)	0%

References

[1] F.T. Pinho, C.F. Li, B.A. Younis, R. Sureshkumar, A low Reynolds number k–e turbulence model for FENE-P viscoelastic fluids, Journal of Non-Newtonian Fluid Mechanics 154 (2008) 89–108.

[2] P.R. Resende, K. Kim, B.A. Younis, R. Sureshkumar, F.T. Pinho, A FENE-P k–e turbulence model for low and intermediate regimes of polymer-induced drag reduction, Journal of Non-Newtonian Fluid   Mechanics 166 (2011) 639–660

[3] G. Iaccarino, E.S.G. Shaqfeh, Y. Dubief, Reynolds-averaged modeling of polymer drag reduction in turbulent flows, Journal of Non-Newtonian Fluid Mechanics 165 (2010) 376–384

[4] J.W. Hoyt, The effect of additives on fluid friction, ASME J. Basic Eng. 94 (1972) 258–285.

[5] J.L. Lumley, Drag reduction by additives, Annu. Rev. Fluid Mech. 1 (1969) 367–384.

[6] J.L. Lumley, Drag reduction in turbulent flow by polymer additives, J. Poly. Sci. 7 (1973) 263–290.

[7] P.S. Virk, Drag reduction fundamentals, AIChE J. 21 (1975) 625–656.

[8] P.S. Virk, An elastic sublayer model for drag reduction by dilute solutions of linear macromolecules, J. Fluid Mech. 45 (1971) 417–440.

[9] M. Tabor, P.G. De Gennes, A cascade theory of drag reduction, Europhys. Lett.2 (1986) 519–522.

[10] F.A. Seyer, A.B. Metzner, Turbulence phenomena in drag reducing systems, AIChE J. 15 (1969) 426– 434.

[11] E.J. Hinch, Mechanical models of dilute polymer solutions in strong flows, Phys. Fluids 20 (1977) S22– S30.

[12] G. Ryskin, Turbulent drag reduction by polymers: a quantitative theory, Phys. Rev. Lett. 59 (1987) 2059– 2062.

[13] R. Sureshkumar, A.N. Beris, R.A. Handler, Direct numerical simulation of the turbulent channel flow of a polymer solution, Phys. Fluids 9 (1997) 743–755.

[14] Y. Dubief, C.M. White, V.E. Terrapon, E.S.G. Shaqfeh, P. Moin, S.K. Lele, On the coherent drag reducing and turbulence enhancing behavior of polymers in wall flows', J. Fluid Mech. 514 (2004) 271– 280.

[15] P.K. Ptasinski, B.J. Boersma, F.T.M. Nieuwstadt, M.A. Hulsen, B.H.A.H. van den Brule, J.C.R. Hunt, Turbulent channel flow near maximum drag reduction: simulations, experiments and mechanisms, J. Fluid Mech. 490 (2003) 251–291.

[16] T. Min, J.Y. Yoo, H. Choi, D.D. Joseph, Drag reduction by polymer additives in a turbulent channel flow, J. Fluid Mech. 486 (2003) 213–238.

[17] C.D. Dimitropoulos, R. Sureshkumar, A.N. Beris, Direct numerical simulation of viscoelastic turbulent channel flow exhibiting drag reduction: the effect of variation of rheological parameters, J. Non-Newton. Fluid Mech. 79 (1998) 433–468.

[18] C.D. Dimitropoulos, Y. Dubief, E.S.G. Shaqfeh, P. Moin, S.K. Lele, Direct numerical simulation of polymer-induced drag reduction in turbulent boundary layer flow, Phys. Fluids 17 (2005) 011705.

[19] R.B. Bird, C.F. Curtiss, R.C. Armstrong, O. Hassager, Dynamics of polymeric liquids Kinetic Theory, vol. 2, 2nd ed., John Wiley & Sons, New York, 1987.

[20] C.F. Li, R. Sureshkumar, B. Khomami, Influence of rheological parameters on polymer induced turbulent drag reduction, J. Non-Newton. Fluid Mech. 140 (2006) 23–40.

[21] M.R. Malin, Turbulent pipe flow of power-law fluids, International Communications in Heat Mass Transfer 24 (7) (1997) 977–988.

[22] M.R. Malin, Turbulent pipe flow of Herschel–Bulkley fluids, International Communications in Heat Mass Transfer 25 (3) (1998) 321–330.

[23] F.T. Pinho, A GNF framework for turbulent flow models of drag reducing fluids and proposal for a k–ε type closure, Journal of Non-Newtonian Fluid Mechanics 114 (2003) 149–184.

 [24] P.R. Resende, M.P. Escudier, F. Presti, F.T. Pinho, D.O.A. Cruz, Numerical predictions and measurements of Reynolds normal stresses in turbulent pipe flow of polymers, International Journal of Heat and Fluid Flow 27 (2006) 204– 219.

[25] R.I. Leighton, D.T. Walker, T.R. Stephens, G.C. Garwood, Reynolds-stress modeling for drag-reducing viscoelastic flow, in: 2003 Joint ASME/JSME Fluids Engineeing Symposium on Friction Drag Reduction, Honolulu, Hawaii, USA, 2003.

 [26] R.B. Bird, P.J. Dotson, N.L. Johnson, Polymer solution rheology based on a finitely extensible bead-spring chain model, J. Non-Newton. Fluid Mech. 7 (1980) 213–235.

[27] H.R. Warner, Kinetic theory and rheology of dilute suspensions of finitely extendible dumbbells, Ind. Eng. Chem. Fundam. 11 (1972) 379–387.

[28] Q. Zhou and R. Akhavan 2003. A comparison of FENE and FENE-P dumbbell and chain models in turbulent flow. J. Non-Newt. Fluid Mech, 109, 115-155.

[29] S.B. Pope. Turbulent Flow. Cambridge University Press, Cambridge, UK, 2001.

[30] H. Tennekes and J.L. Lumley. A First Course in Turbulence. The MIT Press, Cambridge, Massachusetts, 1972.

[31] L. Davidson. Transport equations in incompressible URANS and LES. Report 2006/01, Div. of Fluid Dynamics, Dept. of Applied Mechanics, Chalmers University of Technology, Goteborg, Sweden, 2006.

[32] W.-H. Cai, F.-C. Li, and H.-N. Zhang. DNS study of decaying homogeneous isotropic turbulence with polymer additives. J. Fluid Mech., 665:334–356, 2010.

[33] C.M. Casciola and E. De Angelis. Energy transfer in turbulent polymer solutions. J. Fluid Mech., 581:419, 2007.

[34] F.S. Lien and P. A. Durbin, Non linear $\kappa-\varepsilon- v^2$ modelling with application to high-lift. In: Proceedings of the Summer Program 1996, Stanford University (1996), pp. 5–22.

[35] VK Gupta, R Sureshkumar, B Khomami, Passive scalar transport in polymer drag-reduced turbulent channel flow. AIChE J., 51 (2005) 1938- 1950.

Appendix (A)

Published k-ε-v^2-f model for turbulent viscoelastic fluids

CrossMark

A viscoelastic $k - \varepsilon - \overline{v^2} - f$ turbulent flow model valid up to the maximum drag reduction limit

M. Masoudian [a], K. Kim [b], F.T. Pinho [a,*], R. Sureshkumar [c,d]

[a] *Transport Phenomena Research Center, Faculty of Engineering, University of Porto, Rua Dr. Roberto Frias s/n, 4200-465 Porto, Portugal*
[b] *Department of Mechanical Engineering, Hanbat National University, 125 Dongseo-daero, Yuseong-gu, Daejeon 305-701, South Korea*
[c] *Department of Biomedical and Chemical Engineering, Syracuse University, NY 13244, USA*
[d] *Department of Physics, Syracuse University, NY 13244, USA*

ARTICLE INFO

ABSTRACT

A tensorially consistent near-wall four equation model is developed to model turbulent flow of dilute polymer solutions. The model is validated up to the maximum drag reduction limit, by utilizing the data obtained from direct numerical simulations using the finitely extensible nonlinear elastic-Peterlin (FENE-P) constitutive model. Eight sets of direct numerical simulation (DNS) data are used to analyze budgets of relevant physical quantities, such as the nonlinear terms in the FENE-P constitutive equation, the turbulent kinetic energy, the wall normal Reynolds stress and dissipation transport. Closures were developed in the framework of the $k - \varepsilon - \overline{v^2} - f$ model for the viscoelastic stress work, the viscoelastic destruction of the rate of dissipation, the viscoelastic turbulent viscosity, and the interactions between the fluctuating components of the conformation tensor and of the velocity gradient tensor terms. Predicted polymer stress, velocity profiles and turbulent flow characteristics are all in good agreement with the literature, from which six independent DNS data sets were used covering a wide range of rheological and flow parameters, including high Reynolds number flows, and showing significant improvements over the corresponding predictions of other existing models.

© 2013 Elsevier B.V. All rights reserved.

1. Introduction

It has been known for quite over 60 years that the addition of polymers to turbulent flows of Newtonian fluids can dramatically reduce the turbulent friction drag up to 80%. Comprehensive reviews of the early literature in this area are given in Hoyt [1], Lumley [2,3] and Virk [4]. Several theories have been proposed to describe the complex mechanism of turbulent drag reduction (DR) in dilute polymer solutions. Lumley [2] proposed a mechanism based on the extension of the polymers, suggesting that the stretching of coiled polymers, in regions with strong deformations such as the buffer layer, increases the effective extensional viscosity. This would dampen small eddies, thicken the viscous sublayer and consequently lead to drag reduction. Lumley also related the onset of drag reduction with the time scale of the polymers becoming larger than the time scale of the flow.

In his extensive experimental data analysis Virk [5] introduced the concept of an "elastic sublayer" between the viscous sublayer and the logarithmic zone where crucial events in drag reduction take place. Virk [5], Castro and Squire [6], and Giles and Pettit [7]

observed an increase in the thickness of the elastic sublayer with drag reduction to eventually fill the whole logarithmic and outer layer regions at maximum drag reduction, thus introducing the concept of maximum drag reduction asymptote. On the other hand, Tabor and de Gennes [8] postulated that drag reduction is caused by the elastic rather than the viscous properties of polymer additives. This idea is supported by experiments showing that drag reduction also occurs albeit by a different amount, when the polymers are injected at the center of the pipe (heterogeneous drag reduction). Their explanation was that the shear waves, caused by the elasticity of the polymers prevented production of turbulent velocity fluctuations at the small scales.

Over the last 15 years, the development of accurate and efficient numerical and experimental methods has made it possible to investigate in detail turbulent DR in dilute polymer solutions [9–12]. It is now generally accepted that DR is associated with inhibition of turbulent motion by the action of polymer additives; the high extensional viscosity of the viscoelastic polymer solutions leads to a reduction in the vortex dynamic activities that are characteristic of turbulence taking place near the wall in the viscous and buffer sublayers. This is essentially in agreement with the original proposals of Lumley [2]. More recently, Kim et al. [13,14] proposed the weakening of hairpin vortices by polymer counter-torques as a key mechanism of DR. The torques created by

* Corresponding author. Tel.: +351 225081597.
  E-mail addresses: mmasoudian@fe.up.pt (M. Masoudian), kkim@hanbat.ac.kr (K. Kim), fpinho@fe.up.pt (F.T. Pinho), rsureshk@syr.edu (R. Sureshkumar).

straining the polymers inherently oppose the rotation of the legs and heads of the hairpin vortices in the log layer as well as the quasi-streamwise vortices in the buffer layer.

Several DNS investigations of fully-developed turbulent channel flow have been carried out to understand the effect of rheological parameters on turbulent structure and statistics [15]. Most of these numerical simulations used constitutive equations based on the FENE-P (finitely extensible nonlinear elastic-Peterlin) model which allows one to probe the effect on the flow of the polymer relaxation time, the chain extensibility and the polymer to solution viscosity ratio on the flow.

DNS simulation of turbulent viscoelastic flow is significantly more expensive than Newtonian DNS for two reasons: first, because of the larger number of primary variables in the former than in the latter and secondly, as DR increases, the near wall streaks become progressively stabilized and elongated, thus requiring the use of longer simulation boxes in particular for high DR values [16]. Consequently, for a given Reynolds number, the CPU-time and memory requirements for DNS of viscoelastic flows are at least one order of magnitude larger as compared to the Newtonian case, and so it is not feasible for most of the engineering purposes. Hence, Reynolds-averaged Navier–Stokes (RANS) type or other computationally less demanding models have to be developed for modeling turbulent flows of dilute polymer solutions in engineering applications.

In an attempt to incorporate viscoelastic fluid rheology into turbulence models for drag reducing fluids, Pinho [17], and Resende et al. [18] developed several first-order turbulence models for a modified version of the generalized Newtonian fluid constitutive equation, where the dependence of strain hardening of the fluid on the third invariant of the rate of deformation tensor was included. This family of models also included an anisotropic version to capture the increased Reynolds stress anisotropy [18], and a second order version, where the Reynolds stress tensor was computed from the corresponding transport equations [19].

Leighton et al. [20] proposed the first turbulence model for polymer flows based on the FENE-P dumbbell constitutive equation model. In their closure, transport equations for the Reynolds and the polymer stresses were added to the mean flow equation and closures for the unknown correlations were developed and the model tested in channel flow, but the model was not made available in the open literature. Pinho et al. [21,22] devised a new RANS model for FENE-P fluids, which is an extension of the low Reynolds number k–ε closure for Newtonian fluids. This model provided closures for various terms of the governing equations, but only worked for low DR. Subsequently, Resende et al. [23] developed several sophisticated and exceedingly complex closures for the nonlinear turbulent term of the conformation tensor equation and improved previous closures of Pinho et al. [21] for the viscoelastic stress work and the viscoelastic turbulent transport of the turbulent kinetic energy (k) extending the model to intermediate DR levels and showing the limitations of a simple k–ε approach to modeling polymer solutions up to high DR. In fact, since turbulence anisotropy increases with DR, the inherent turbulence isotropy of the k–ε model does not allow the simultaneous accurate prediction of mean velocity, turbulent kinetic energy and its rate of dissipation at high DR.

Iaccarino et al. [24] introduced a $k - \varepsilon - \overline{v^2} - f$ model for fully developed channel flow, which is capable of predictions over the whole range of DR. The concept of turbulent polymer viscosity (or viscoelastic eddy viscosity) was used to account for the combined effects of turbulence and viscoelasticity on the polymer extra stress tensor term in the momentum equation. The turbulent polymer viscosity was made to depend on the turbulent kinetic energy, the polymer relaxation time and the trace of conformation tensor, an idea that is adopted here with a new improved closure. The

model of the nonlinear terms in the conformation tensor equation relied on the turbulent dissipation rate, but the main characteristic of Iaccarino et al.'s model [24], imported from the corresponding Newtonian model, was the ability to incorporate into the Reynolds stress tensor closure the wall damping effect upon the wall normal turbulence via the scalar $\overline{v^2}$ and the role of pressure strain. Both of these quantities are significantly modified by polymer additives and enhance turbulence anisotropy. However, although their model predicts accurately the amount of drag reduction, their predictions of the polymer shear stress in the Reynolds-averaged momentum, of the budgets of the turbulent kinetic energy and of the evolution equation for the conformation tensor are not in agreement with DNS results. In this work we aim to address these shortcomings by presenting a new $k - \varepsilon - \overline{v^2} - f$ model for FENE-P fluids and test it in fully-developed turbulent channel flow, which is essential to a future extension to other flows.

The single-point turbulence model developed here is based on the time-averaged governing equations for viscoelastic fluids presented by Dimitropoulos et al. [25]. An important contribution of the present work is the development of new closures for the nonlinear fluctuating terms appearing in the FENE-P rheological constitutive equation, and for the polymer stress work terms in the k and $\overline{v^2}$ transport equations. The model is assessed against different sets of DNS data covering a wide range of flow and fluid conditions quantified by the Weissenberg number (Wi), Reynolds number (Re) and maximum polymer extensibility (L^2). The paper is organized as follows: Section 2 introduces the instantaneous and time-averaged governing equations and identifies the viscoelastic terms requiring modeling. In Section 3, the turbulent closures are developed and Section 4 presents model predictions for fully developed turbulent channel flow over the whole range of DR. Conclusions are offered in Section 5.

2. Governing equations

In what follows, upper-case letters or overbars denote Reynolds-averaged quantities and lower-case letters or primes denote fluctuating quantities. A hat denotes an instantaneous quantity. In this work steady flows are dealt with and the reader should be aware that the terms "time-averaging" and "Reynolds-averaging" are used indiscriminately to denote "Reynolds-averaging".

2.1. Continuity and momentum equations

The Reynolds-averaged equations appropriate for incompressible flow of FENE-P fluids are:
continuity:

$$\frac{\partial U_i}{\partial x_i} = 0 \tag{1}$$

and momentum:

$$\rho \frac{\partial U_i}{\partial t} + \rho U_k \frac{\partial U_i}{\partial x_k} = -\frac{\partial \overline{P}}{\partial x_i} - \frac{\partial}{\partial x_k}(\overline{\rho u_i u_k}) + \frac{\partial \overline{\tau}_{ik}}{\partial x_k} \tag{2}$$

where $\overline{\tau}_{ik}$ is the time-averaged extra stress tensor, U_i is the mean velocity, $\overline{P}$ is the mean pressure, ρ is the fluid density and $-\rho \overline{u_i u_k}$ is the Reynolds stress tensor. The extra stress tensor $\overline{\tau}_{ij}$ describes the rheology of the fluid and is given in Eq. (3) as the sum of a Newtonian solvent contribution of viscosity η_S with a polymeric contribution $\overline{\tau}_{ij,p}$ described by the FENE-P rheological constitutive model:

$$\overline{\tau}_{ij} = 2\eta_s S_{ij} + \overline{\tau}_{ij,p} \tag{3}$$

where S_{ij} is the rate of strain tensor defined as:

$$S_{ij} = \frac{1}{2}\left(\frac{\partial U_i}{\partial x_j} + \frac{\partial U_j}{\partial x_i}\right) \tag{4}$$

In Eqs. (2) and (3) the Reynolds stress and the time-averaged polymer stress need approximations. The former can be calculated by models developed for Newtonian fluids but modified to account for the effects of viscoelasticity, whereas the latter must be calculated with the Reynolds-averaged rheological constitutive equation.

2.2. Constitutive equation

To develop a model for $\overline{\tau}_{ij,p}$, we start with the instantaneous FENE-P equation for the polymeric stress [26,27]. The instantaneous polymeric contribution to the total extra stress is given as an explicit function of the instantaneous conformation tensor $\hat{c}_{ij}$

$$\hat{\tau}_{ij,p} = \frac{\eta_p}{\lambda} [f(\hat{c}_{kk})\hat{c}_{ij} - f(L)\delta_{ij}] \tag{5}$$

where the different $f(\hat{c}_{kk})$ and $f(L)$ functions take here the forms used by Li et al. [16,28] and are given by

$$f(\hat{c}_{kk}) = \frac{L^2 - 3}{L^2 - \hat{c}_{kk}} \quad \text{and} \quad f(L) = 1 \tag{6}$$

where L denotes the maximum dimensionless extensibility of the model dumbbell. Other functions are discussed in [29]. The required conformation tensor obeys a hyperbolic differential equation of the form:

$$f(\hat{c}_{kk})\hat{c}_{ij} + \lambda \left(\frac{\partial \hat{c}_{ij}}{\partial t} + \hat{u}_k \frac{\partial \hat{c}_{ij}}{\partial x_k} - \hat{c}_{jk} \frac{\partial \hat{u}_i}{\partial x_k} - \hat{c}_{ik} \frac{\partial \hat{u}_j}{\partial x_k} \right) = f(L)\delta_{ij} \tag{7}$$

Using Eqs. (5) and (7) can be alternatively written as

$$\left(\frac{\partial \hat{c}_{ij}}{\partial t} + \hat{u}_k \frac{\partial \hat{c}_{ij}}{\partial x_k} - \hat{c}_{jk} \frac{\partial \hat{u}_i}{\partial x_k} - \hat{c}_{ik} \frac{\partial \hat{u}_j}{\partial x_k} \right) = -\frac{\hat{\tau}_{ij,p}}{\eta_p} \tag{8}$$

The terms in the parenthesis in Eqs. (7) and (8) denote Oldroyd's upper convective derivative of the instantaneous conformation tensor. The first two terms represent the local and advective derivatives (together they form the material derivative) and the other two terms account for the distortion of c_{ij} by the instantaneous flow. The other parameters of the polymer constitutive equation are the relaxation time of the fluid λ and the polymer viscosity coefficient η_p.

Reynolds-averaging the above equations, the time-averaged polymer stress $\overline{\tau}_{ij,p}$ is obtained:

$$\overline{\tau}_{ij,p} = \frac{\eta_p}{\lambda} [f(C_{kk})C_{ij} - f(L)\delta_{ij}] + \frac{\eta_p}{\lambda} \overline{f(C_{kk} + c_{kk})c_{ij}} \tag{9}$$

where the last term on the right hand side also needs an approximation. The time-averaged form of the conformation tensor evolution equation is:

$$\overset{\nabla}{C}_{ij} + \overline{u_k \frac{\partial c_{ij}}{\partial x_k}} - \left(\overline{c_{jk} \frac{\partial u_i}{\partial x_k}} + \overline{c_{ik} \frac{\partial u_j}{\partial x_k}} \right) = -\frac{\overline{\tau}_{ij,p}}{\eta_p} \tag{10}$$

which after substitution of Eq. (9), becomes:

$$\lambda \overset{\nabla}{C}_{ij} + \lambda \left(\overline{u_k \frac{\partial c_{ij}}{\partial x_k}} - \left(\overline{c_{jk} \frac{\partial u_i}{\partial x_k}} + \overline{c_{ik} \frac{\partial u_j}{\partial x_k}} \right) \right)$$
$$= -[f(C_{kk})C_{ij} - f(L)\delta_{ij} + \overline{f(C_{kk} + c_{kk})c_{ij}}] \tag{11}$$

On the left hand side of Eqs. (10) and (11), the mean flow advective term contained within the Oldroyd derivative of C_{ij} (denoted by $\overset{\nabla}{C}_{ij}$) vanishes for fully developed channel flow. The mean flow distortion term of $\overset{\nabla}{C}_{ij}$ is M_{ij} and is given by:

$$M_{ij} = \left(C_{jk} \frac{\partial U_i}{\partial x_k} + C_{ik} \frac{\partial U_j}{\partial x_k} \right) \tag{12}$$

M_{ij} is non-zero, but it needs no closure. The remaining two terms are related to turbulence correlations and, following the analysis and nomenclature of Li et al. [28] and Housiadas et al. [30], they are labeled as

$$CT_{ij} = -\overline{u_k \frac{\partial c_{ij}}{\partial x_k}} \tag{13}$$

which represents the contribution to the advective transport of the conformation tensor by the fluctuating velocity field, and

$$NLT_{ij} = \overline{c_{jk} \frac{\partial u_i}{\partial x_k}} + \overline{c_{ik} \frac{\partial u_j}{\partial x_k}} \tag{14}$$

which accounts for the interactions between the fluctuating components of the conformation tensor and of the velocity gradient tensor. This term originates from the Oldroyd derivative and is the fluctuating counterpart of M_{ij}. Both CT_{ij} and NLT_{ij} require closure approximations.

In this study we investigate fully developed channel flow of FENE-P fluids over a wide range of conditions as described in Table 1, which lists the DNS data sets. All DNS cases correspond to $\beta = 0.9$, the Reynolds number $Re_{\tau 0}$ is defined as $Re_{\tau 0} \equiv h \, U_\tau / v_o$ based on the friction velocity (U_τ), the channel half-height (h) and the zero shear-rate kinematic viscosity of the solution, i.e., the sum of the kinematic viscosities of the solvent and polymer $v_0 = v_p + v_s$. All kinematic viscosities are defined with the total solution density. The Weissenberg number is $Wi_{\tau 0} \equiv \lambda U_\tau^2 / v_0$ and β is the ratio between the solvent kinematic viscosity and the zero shear-rate kinematic viscosity of the solution, $\beta \equiv v_s / v_0$. A semi-implicit method is used for time-integration of the governing equations. In space, a spectral method is used with Fourier representations in the streamwise and spanwise directions, and Chebyshev expansion in the wall-normal direction. To achieve stable numerical integration of Eq. (8), a stress diffusion term ($\kappa \partial^2 \hat{c}_{ij} / \partial x_k^2$) is introduced, where κ denotes a constant, isotropic, artificial numerical diffusivity. As in earlier studies [10,14], the dimensionless artificial numerical diffusivity is taken to be $\kappa / h u_\tau \sim O(10^{-2})$. Periodic boundary conditions are applied in the streamwise (x) and spanwise (z) directions, and the no-slip boundary condition is imposed on velocity at the solid walls. Details of the numerical approaches used in this work can be found in [16].

In normalizing the governing equations and inherently the various physical quantities, the velocity scale is taken to be the friction velocity (leading to the use of superscript +), the length scale is either the channel half-height ($x_i = x_i^* h$) or the viscous length ($x_i = x_i^+ v_o / U_\tau$), leading to superscripts * and +, respectively. When mixing the two types of normalization, i.e. using wall/viscous and physical quantities, the superscript used is *, e.g. $M_{ij} = M_{ij}^* U_\tau^2 / v_0$. The conformation tensor is already in dimensionless form.

2.3. Reynolds stresses

To compute the Reynolds stress tensor, we adopt Boussinesq's turbulent stress–strain relationship:

$$-\rho \overline{u_i u_j} = 2\rho v_T S_{ij} - \frac{2}{3}\rho k \delta_{ij} \tag{15}$$

where v_T is the eddy viscosity and k is the turbulent kinetic energy, $\overline{u_i u_i}/2$. The eddy viscosity is modeled according to the $k - \varepsilon - \overline{v^2} - f$ model [31]. This particular choice is justified by the fact that the polymer drag reduction is mostly a near wall phenomenon, and it requires a modification to the turbulence redistribution mechanism. This model of Lien and Durbin [31] represents a comprehensive and accurate approach to capture these aspects of turbulent boundary layers within a Boussinesq framework. Durbin's original proposal [32] for a near-wall eddy viscosity model is inspired by the physics of the full Reynolds stress transport model, but retains only the wall-normal fluctuating velocity variance, $\overline{v^2}$, and its

Table 1
DNS parameters.

Case	$Re_{\tau 0}$	Domain size	Nodes (N_x, N_y, N_z)	Artificial diffusivity (κ/hu_τ)	L^2	$Wi_{\tau 0}$	DR (%)
(A)	395	L_x:8πh, L_z:πh	$512 \times 129 \times 128$	0.02	900	25	18
(B)	395	L_x:8πh, L_z:πh	$512 \times 129 \times 128$	0.02	900	100	37
(C)	395	L_x:16πh, L_z:πh	$1024 \times 129 \times 128$	0.025	3600	100	51
(D)	395	L_x:16πh, L_z:πh	$1024 \times 129 \times 128$	0.025	14,400	100	63
(E)	180	L_x:7h, L_z:πh	$64 \times 97 \times 64$	0.02	900	25	19
(F)	180	L_x:14h, L_z:πh	$128 \times 97 \times 64$	0.02	900	100	38
(G)	180	L_x:14h, L_z:πh	$128 \times 97 \times 64$	0.02	3600	100	54
(H)	180	L_x:28h, L_z:πh	$128 \times 97 \times 64$	0.02	14,400	100	71

source, kf, representing the redistribution by pressure fluctuations. Then, in the classical closure for the eddy viscosity ($v_T \propto k^2/\varepsilon$) the wall damping effect is obtained by substituting one instance of k by $\overline{v^2}$ as:

$$v_T = C_\mu \overline{v^2} T_t \qquad (16)$$

where T_t is the turbulent time scale defined as:

$$T_t = \max\left\{\frac{k}{\varepsilon}, 6\sqrt{\frac{v}{\varepsilon}}\right\} \qquad (17)$$

Thus, the turbulence model for Newtonian fluids has three transport equations for k, ε and $\overline{v^2}$, and one elliptic equation for f, and it accurately reproduces the parabolic decay of $\overline{v^2}/k$ down to the solid wall without introducing the wall-distance or low-Reynolds number damping functions in the eddy viscosity and k–ε equations, which would then need to be modified to account for viscoelastic fluids. The absence of these damping functions is a major strength of this type of closures. However, most $\overline{v^2} - f$ variants suffer from numerical stiffness making them impractical for industrial or unsteady RANS applications, while the one version available in major commercial codes often tends to lead to unrealistic solutions. Lien and Durbin [31] proposed a variant to address these shortcomings.

In the $\overline{v^2} - f$ model suggested by Lien and Durbin [31], the scalar $\overline{v^2}$, and its source term f, are retained as variables in addition to the traditional k and ε quantities. The turbulent kinetic energy transport equation is derived formally from the Reynolds-averaged momentum equation and, therefore, in this case contains extra terms originating from the polymer stresses.

The transport equations for the turbulent kinetic energy and its dissipation rate share similarities with the classical k–ε model equations, but contain additional terms for viscoelastic fluids, as reported by Pinho et al. [21]. The transport equation of k for turbulent flow of viscoelastic fluids is

$$U_j \frac{\partial k}{\partial x_j} = P_k - \varepsilon + \frac{\partial}{\partial x_j}\left(\left(v + \frac{v_T}{\sigma_k}\right)\frac{\partial k}{\partial x_j}\right) - \overline{\left(\tau_{ij}^p \frac{\partial u_i}{\partial x_j}\right)}$$
$$+ \frac{\partial}{\partial x_j}\left(\overline{\tau_{ij}^p u_i}\right) \qquad (18)$$

Except for the last two terms on the right hand side, the other terms are classical terms appearing in Newtonian fluid models and represent the advection of k, turbulence production by the mean strain ($P_k = 2v_T S_{ij}^2$), viscous dissipation by the solvent, molecular diffusion and turbulent diffusion. The two viscoelastic terms require closure and represent the viscoelastic turbulent transport ($Q_p \equiv \partial(\overline{\tau_{ij}^p u_i})/\partial x_j$) and the viscoelastic stress work ($\varepsilon_p \equiv \overline{\tau_{ij}^p \partial u_i/\partial x_j}$).

The balance of turbulent kinetic energy is plotted in Fig. 1 for low (18%) and high (63%) drag reductions using normalization by wall quantities (e.g. $\varepsilon = \varepsilon^+ u_\tau^4/v_0$). The turbulent kinetic energy budgets in Fig. 1 show that the qualitative behavior of the various terms is not affected by the level of drag reduction, although the thickening of the sublayer is clearly noticeable from the shift of the peak of kinetic energy production away from the wall. As for
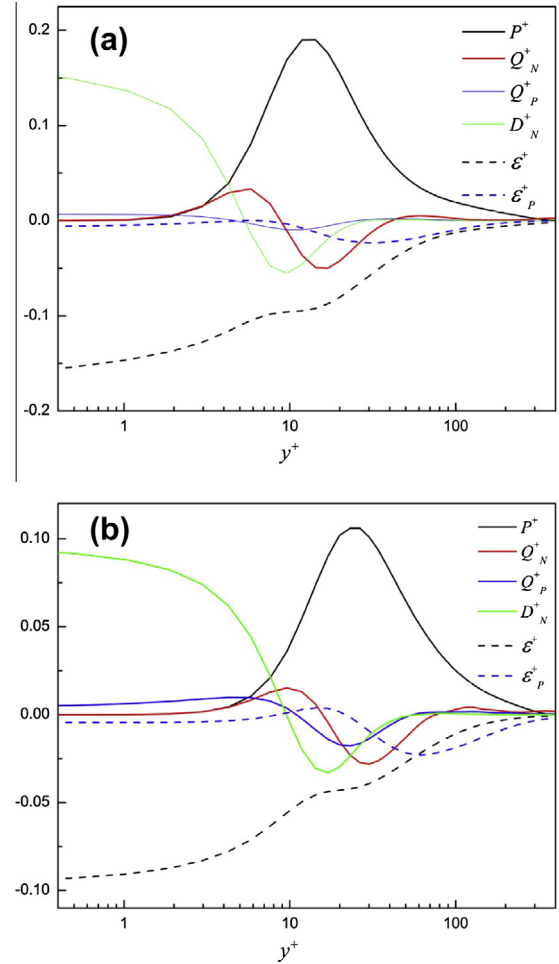

Fig. 1. Balance of turbulent kinetic energy at $Re_{\tau 0}$ = 395 (a) case A, and (b) case D.

a Newtonian fluid, the main contributions in the log-law region are from the production of k on one side, and the dissipations by the Newtonian solvent and by the viscoelastic stress work on the other. This is why the viscous dissipation due to the solvent is lower in the viscoelastic case than for a Newtonian fluid at the same Reynolds number. Well inside the viscous sublayer molecular diffusion takes over the role of production, and dissipation by the solvent is greater than the viscoelastic stress work. The viscoelastic turbulent transport term is usually small and only relevant within the buffer layer, but even there smaller than the turbulent diffusion (D_N), hence this term will not have a dramatic impact on model predictions.

The dissipation by the Newtonian solvent (ε) appearing on the right hand side of Eq. (18), is obtained from its own transport equation:

$$U_j \frac{\partial \varepsilon}{\partial x_j} = \frac{C_{\varepsilon 1} P_k - C_{\varepsilon 2} \varepsilon}{T_t} + \frac{\partial}{\partial x_j}\left(\left(v + \frac{v_T}{\sigma_\varepsilon}\right)\frac{\partial \varepsilon}{\partial x_j}\right) - E_p \tag{19}$$

Here, all terms are conceptually identical to those for a Newtonian fluid except for the last term (E_p) representing the viscoelastic contribution to the transport equation of ε. The definition of E_p was derived by Pinho et al. [21] and is given by:

$$E_p = 2v_s \frac{\eta_p}{\lambda(L^2 - 3)} \overline{\frac{\partial u_i}{\partial x_m} \frac{\partial}{\partial x_k}\left\{\frac{\partial}{\partial x_m}\left[f(C_{mm})f(\hat{c}_{pp})c'_{qq}C_{ik}\right]\right\}} \tag{20}$$

This term is clearly nonlinear and a closure is needed for its calculation.

The other two equations needed to compute the eddy viscosity (cf. Eq. (16)) are the transport equation for the scalar $\overline{v^2}$, which is derived from the transport equation for the wall normal turbulent fluctuations according to [24], and the equation for the turbulence energy redistribution process (f) that plays a crucial role in producing $\overline{v^2}$ (cf. Eq. (22)). In the context of a second order model for the full Reynolds stress tensor such role is played by the pressure-strain correlations from which the f-equation[1] gets derived. The equations for $\overline{v^2}$ and f are given below:

$$U_j \frac{\partial \overline{v^2}}{\partial x_j} = kf + \frac{\partial}{\partial x_j}\left(\left(v + \frac{v_T}{\sigma_k}\right)\frac{\partial \overline{v^2}}{\partial x_j}\right) - 6\frac{\varepsilon}{k}\overline{v^2} - \varepsilon_{p,yy} + Q_{p,yy} \tag{21}$$

$$f - L_t^2 \frac{\partial^2 f}{\partial x_j \partial x_j} = C_1 \frac{\left(\frac{2}{3} - \frac{\overline{v^2}}{k}\right)}{T_t} + C_2 \frac{P_k}{k} - 5\varepsilon \frac{\overline{v^2}}{k} + \Phi_{yy}^p \tag{22}$$

where the eddy viscosity and time scale are given in Eqs. (16) and (17), and the length scale is defined as:

$$L_t^2 = C_L^2 \max\left\{\frac{k^3}{\varepsilon^2}, C_\eta^2 \sqrt{\frac{v^3}{\varepsilon}}\right\} \tag{23}$$

As reported in [31] the coefficients appearing in the above equations are: $C_\mu = 0.19, \sigma_k = 1, \sigma_\varepsilon = 1.3, C_{s1} = 1.4[1 + 0.05\sqrt{k/\overline{v^2}}]$, $C_{s2} = 1.9, C_1 = 1.4, C_2 = 0.3, C_L = 0.23, C_\eta = 70$. The transport equation for $\overline{v^2}$, a scalar representing the local wall-normal Reynolds stress, is also modified relative to the corresponding Newtonian equation due to the presence of polymer additives in a similar manner to the k transport equation. The last two terms in Eq. (21) are the viscoelastic turbulent transport of $\overline{v^2}$ ($Q_{p,yy}$) and the viscoelastic stress work of $\overline{v^2}$ ($\varepsilon_{p,yy}$), and correspondingly they also need closures. The qualitative behavior of $\varepsilon_{p,yy}$, $Q_{p,yy}$, and kf depicted in Fig. 2 shows that for the low drag reduction case the peaks of kf and $\varepsilon_{p,yy}$ occur close to the wall, and then the quantities fall significantly by moving away from the wall. On the other hand for the high drag reduction case the maximum values of the dimensionless quantities are much lower than at low DR and sharp peaks are no longer observed near the wall. Instead, there is a wide region where those quantities are close to the maximum. In addition, when increasing DR the ratio $\varepsilon_{p,yy}/(kf)$ increases, i.e., the wall normal viscoelastic stress work becomes an increasing proportion of kf and this suggest that wall normal velocity fluctuations tend to decrease as DR increases. The last term in Eq. (22), Φ_{yy}^p is representing the viscoelastic contribution to the f equation. Note that subscript yy used in this work denotes the wall-normal direction.

3. Development of closures

In this section closures are developed for all unknown turbulent cross-correlations identified in the previous section. All closures

---

Fig. 2. DNS data for the normalized budgets of $\overline{v^2}$ for cases A (LDR, DR = 18%) and D (HDR, DR = 63%) at $Re_{\tau 0} = 395$.
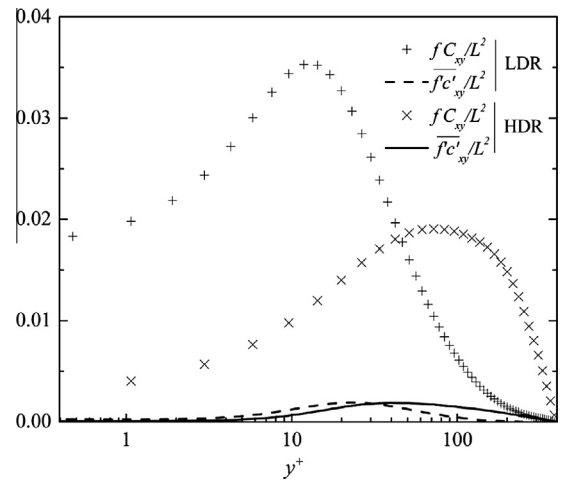
Fig. 3. Comparison between $\overline{f(C_{kk} + c_{kk})c_{xy}}$ and $f(C_{kk})C_{xy}$ for cases A (LDR, DR = 18%) and D (HDR, DR = 63%) at $Re_{\tau 0} = 395$.

are developed on the basis of the DNS data case (B) ($Re_{\tau 0} = 395$ and $DR = 37\%$ in Table 1) and subsequently compared with the other DNS data sets.

3.1. A model for the time-averaged polymer constitutive equation

For fully developed channel flow the polymer shear stress given by the FENE-P constitutive equation reduces to:

$$\overline{\tau}_{xy,p} = \frac{\eta_p}{\lambda}[f(C_{kk})C_{xy} - f(L)\delta_{ij}] + \frac{\eta_p}{\lambda}\overline{f(C_{kk} + c_{kk})c_{xy}} \tag{24}$$

which contains a nonlinear term, $\overline{f(C_{kk} + c_{kk})c_{xy}}$. This quantity is compared with its mean value $f(C_{kk})C_{xy}$ in Fig. 3 for both low (case A) and high (case D) drag reductions, and confirms the assertion that, in Eq. (24), it is justifiable to neglect the last term on the right-hand-side by comparison with the first term, as also found previously [24,21]. Consequently for fully developed channel flow the polymer shear stress can in principle be calculated by:

$$\overline{\tau}_{xy,p} = \frac{\eta_p}{\lambda}f(C_{kk})C_{xy} \tag{25}$$

Eq. (25) implies that in fully-developed turbulent channel flow of viscoelastic fluids described by the FENE-P model we need the trace of the conformation tensor (C_{kk}) and the mean shear polymer conformation component (C_{xy}) to calculate the polymer shear stress.

---

[1] Note that f and $f(C_{ij})$ denote two different unrelated quantities: f is the velocity fluctuation redistribution function of the turbulence model (Eq. (22)), whereas $f(C_{ij})$ is the function of the conformation tensor in the FENE-P model (Eq. 6).
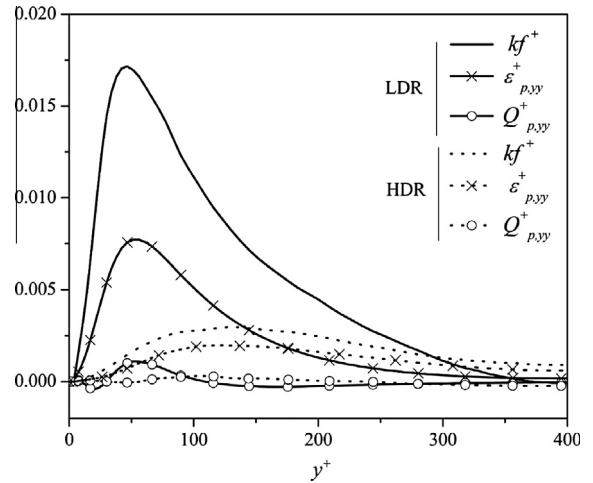
Still the polymer stress depends on turbulent quantities since the conformation tensor is highly dependent on turbulent flow characteristics as shown by Eqs. (11)–(14). The consequence of that cascade of dependencies is that small differences in the closures of those quantities result in inaccurate prediction of the polymer stress. Hence, instead of using Eq. (25) Iaccarino et al. [24] introduced the concept of viscoelastic kinematic viscosity ($v_{T,p}$) in order to directly account for the effect of turbulence on C_{ij}. They related the viscoelastic kinematic viscosity to the turbulent kinetic energy, and proposed a closure for $v_{T,p}$ and $\overline{\tau}_{xy,p}$ as:

$$\overline{\tau}_{xy,p} = \frac{\rho}{f(C_{kk})}(v_p + v_{T,p})S_{xy} \quad \text{where} \quad v_{T,p} = b\lambda k, \quad b = 0.1 \quad (26)$$

We follow some of those ideas, but model the Reynolds-averaged polymer shear stress differently and as follows. In order to account for the variations in the mean polymer shear stress we utilized the trace of the C_{ij} tensor, as in Eq. (25). However, to capture the effect of turbulence upon C_{ij} we followed the concept of turbulent kinematic viscosity ($v_{T,p}$) introduced by Iaccarino et al. [24]. This is something like introducing a concept of viscoelastic turbulent Prandtl number, which is a decomposition of total viscoelastic momentum diffusivity into molecular and turbulent contributions. The turbulent viscoelastic kinematic viscosity ($v_{T,p}$) describes the effect of the turbulent fluctuations on the polymer stresses, and relies on a Boussinesq-like relationship meaning an alignment of the viscoelastic stresses with the mean strain (consistent with a dumbbell spring). Fig. 4 compares DNS data for the kinematic eddy viscosity, the viscoelastic kinematic viscosity ($v_{T,p} = \overline{\tau}_{xy,p}/(\rho dU_x/dy)$) and the closure developed in [24]. The behavior of the turbulent viscoelastic kinematic viscosity, $v_{T,p}$, can be rationalized as follows. In the viscous sublayer ($y^+ < 5$), where the turbulence is severely dampened, it is possible to calculate the polymer stress neglecting any effect of turbulence upon the constitutive equation, i.e., by using the laminar constitutive equation. The polymer stress in fully-developed laminar channel flow has the exact solution given by [21] as:

$$\tau_{xy,lam,p} = \frac{\rho v_p}{f(C_{kk})}\frac{dU_x}{dy} \quad (27)$$

Eq. (27) is sufficient to describe the polymer stress in the viscous sublayer ($y^+ < 5$ region) while ensuring the compatibility of the polymer stresses in laminar flows. As depicted in Fig. 4 the turbulent viscoelastic viscosity attains its maximum away from the wall and then decreases slowly towards the centerline as is also the case with the eddy viscosity (v_T). Moreover, a correct closure for the
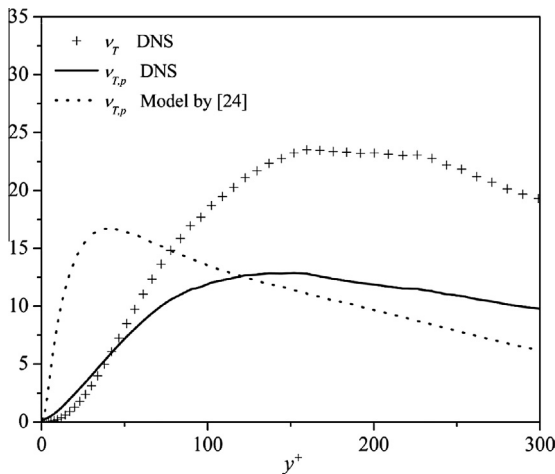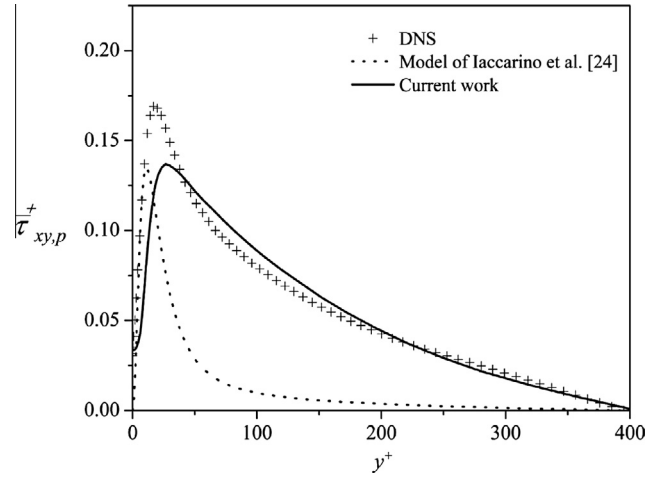

Fig. 5. Comparison between current model for the polymer mean shear stress, the model of [24] and DNS data for case B (DR = 37% and $Re_{\tau 0}$ = 395).
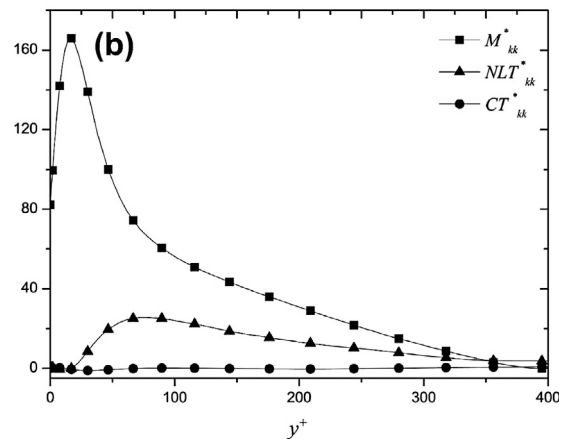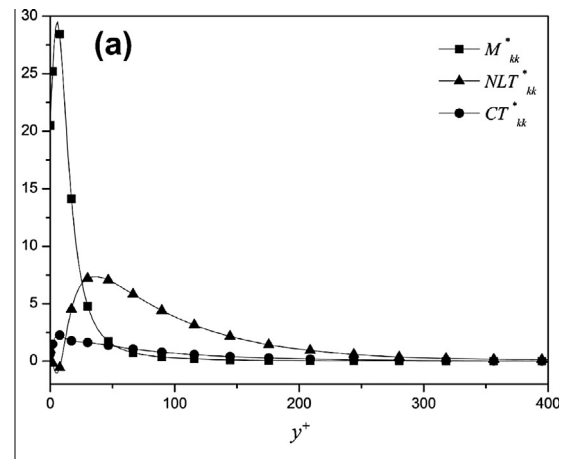

Fig. 6. Contributions to the trace of the conformation tensor (Eq. (31)) in fully developed channel flow for (a) case A, and (b) case D.

polymer shear stress should naturally follow the dynamics imposed by the constitutive FENE-P Eq. (25) in regard to $f(C_{kk})$ and the polymer relaxation time. By analyzing the DNS data and experimental results of [12], we observed that away from the wall there is a partial correspondence between the eddy viscosity and the viscoelastic eddy viscosity and consequently we propose a closure for the viscoelastic turbulent viscosity in the whole domain as:
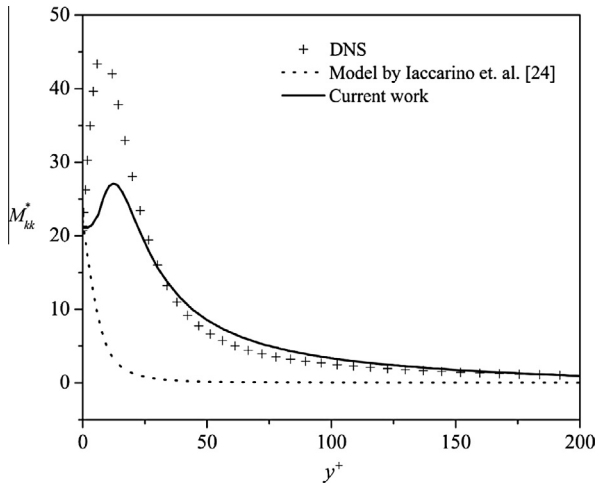

Fig. 4. Variation of $v_{T,p}$ and v_T for DR = 37% (case B in Table 1) across the channel and comparison with the model of $v_{T,p}$ developed by [24].

Fig. 7. Comparison between the predicted M_{kk} by current method with the model of [24], and DNS data for case B.

$$v_{T,p} = \left(\frac{v_p}{f(C_{kk})} + a_1 \sqrt{L^2/Wi_{\tau 0}} f(C_{kk}) v_T \right) \quad (28)$$

and the time averaged polymer shear stress becomes:

$$\overline{\tau}_{xy,p} = \rho \left(\frac{v_p}{f(C_{kk})} + a_1 \sqrt{L^2/Wi_{\tau 0}} f(C_{kk}) v_T \right) \frac{dU_x}{dy}, \quad (29)$$

where the first term on the right hand side dominates in the near wall region and the second term captures the effect of turbulence far from the wall. By utilizing the turbulent term of $v_{T,p}$, the turbulent viscoelastic Prandtl number ($Pr_{T,p}$) is defined as: $Pr_{T,p} = a_1 \sqrt{L^2/Wi_{\tau 0}} f(C_{kk})$. The model for the kinematic turbulent viscoelastic viscosity developed with data for case B (DR = 37%) is compared in Fig. 5, in terms of the polymer stress, with DNS data and the model of Eq. (26) previously proposed by Iaccarino et al. [24]. While this latter model describes well the rise of the shear stress very close to the wall it severely under-predicts the polymer stress away from the wall, a feature corrected by the proposed closure.

To compute the polymer stress according to the model of Eq. (29) we also need the extension of the chains via C_{kk} and this can be computed directly via the corresponding Reynolds-averaged equation, which is obtained as the trace of the Reynolds-averaged conformation Eq. (11):
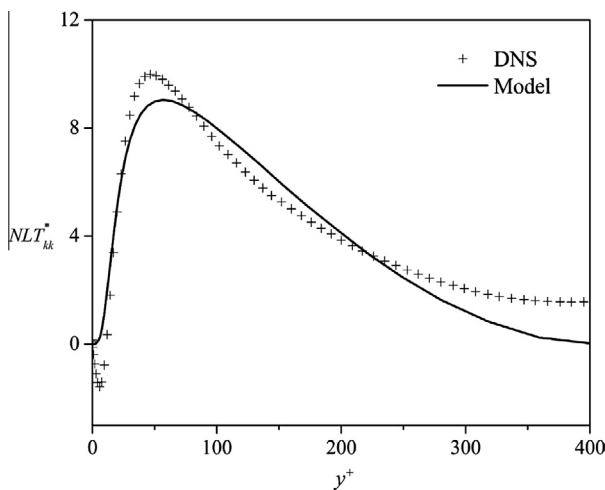

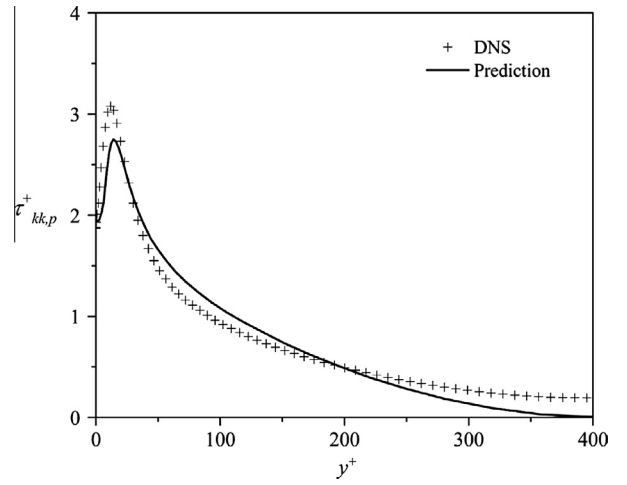**Fig. 8.** Comparison between predicted NLT_{kk} and DNS data for case B.

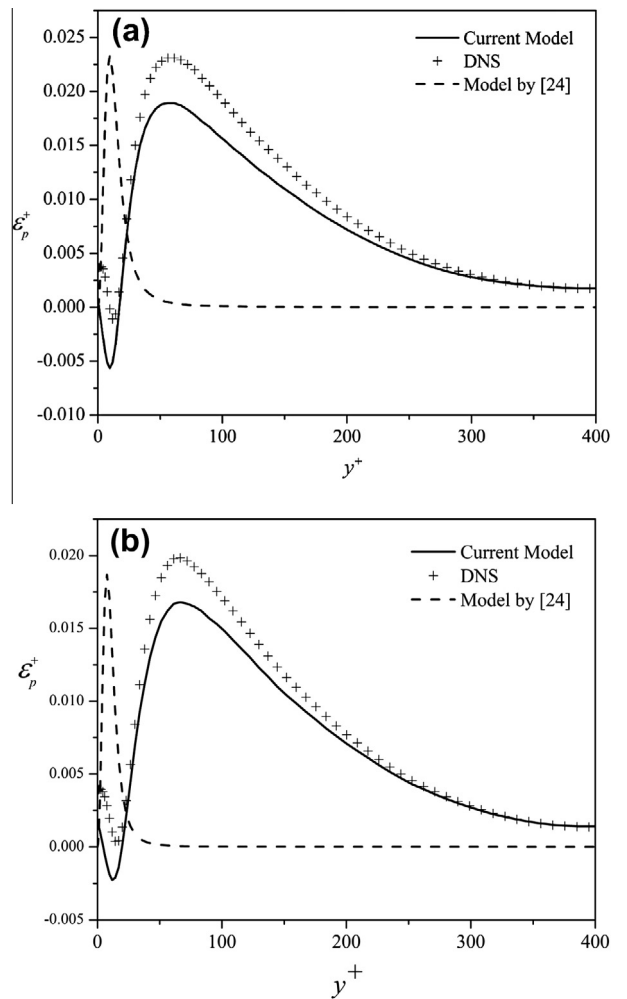**Fig. 9.** Comparison between predicted and DNS data of $\tau_{kk,p}$ for case B.

Fig. 10. Comparison between current model for ε_p against DNS data and the model of [24] for (a) case C, and (b) case D.

$$M_{kk} + NLT_{kk} + CT_{kk} + \frac{1}{\lambda}(3 - f(C_{kk})C_{kk}) = 0 \quad (30)$$

In Eq. (30) M_{kk} is the trace of the mean flow distortion term of $\overset{\triangledown}{C}_{ij}$, NLT_{kk} accounts for the interactions between the fluctuating

components of the conformation and velocity gradient tensors, and CT_{kk} is the contribution to the transport of the conformation tensor by the fluctuating advection.

Fig. 6 compares the first three terms on the left-hand-side of Eq. (30) for low (case A) and high (case D) drag reductions, showing CT_{kk} to be negligible regardless of the amount of DR, in agreement with the findings of Housiadas et al. [30] and Li et al. [16]. In contrast, NLT_{kk} is not negligible, and its closure constitutes a main task in this work. Apart from NLT_{kk}, the other main contribution comes from the exact mean flow term (M_{kk}), especially in the viscous sublayer and buffer layer.

Provided the model for $v_{T,p}$ is robust, M_{kk} is easily computed from its definition. For fully-developed flow we have $M_{yy} = M_{zz} = 0$ and

$$M_{xx} = 2C_{xy}\frac{dU}{dy} \rightarrow M_{kk} = 2\left(\frac{\lambda\overline{\tau}_{xy,p}}{\eta_p f(C_{kk})}\frac{dU}{dy}\right) \qquad (31)$$

Fig. 6 shows that this term is an important term in Eq. (30). Although M_{kk} is exact, Iaccarino et al. [24] proposed the following model to compute it:

$$M_{kk} = \frac{2\lambda}{f^2(C_{kk})}\left(\frac{dU_x}{dy}\right)^2 \qquad (32)$$

which is the exact solution for laminar channel flow. Fig. 7 compares the predictions of M_{kk} using our method (Eq. (31)) and the model of Iaccarino et al. [24] (Eq. (32)) and includes also the corresponding DNS data. The use of the exact definition of the M_{kk}, based on our model for the turbulent polymer viscosity is able to predict better the distribution of M_{kk} all across the channel.

NLT_{kk} accounts for the interactions between the fluctuating components of the conformation tensor and of the velocity gradient tensor. For low and intermediate DR a closure for NLT_{ij} was derived by Resende et al. [23], but that is a very complex model. An alternative simpler closure had been previously derived by Pinho et al. [21,22], but in this work we develop a specific model for the trace NLT_{kk}, simpler than any of the previous existing closures, and here NLT_{kk} is related to its mean value (M_{kk}) and the eddy viscosity via:

$$NLT_{kk} = a_2 M_{kk}\frac{v_T}{v_o} \qquad (33)$$

Mathematically NLT_{kk} originates from the Oldroyd derivative and it is the fluctuating counterpart of M_{kk}. The closure of Eq. (33) was developed after an extensive analysis of DNS data and the constant coefficient appearing in it was fixed on the basis of the data for case
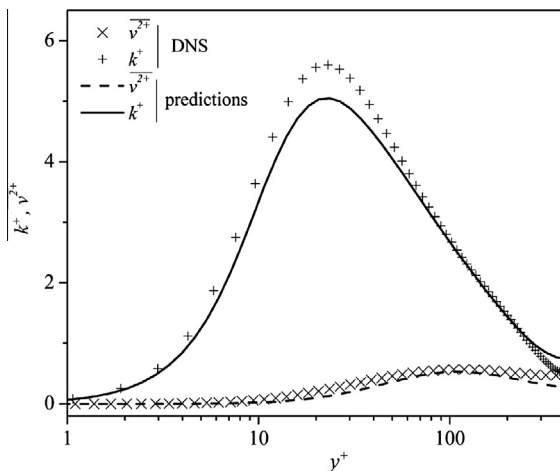

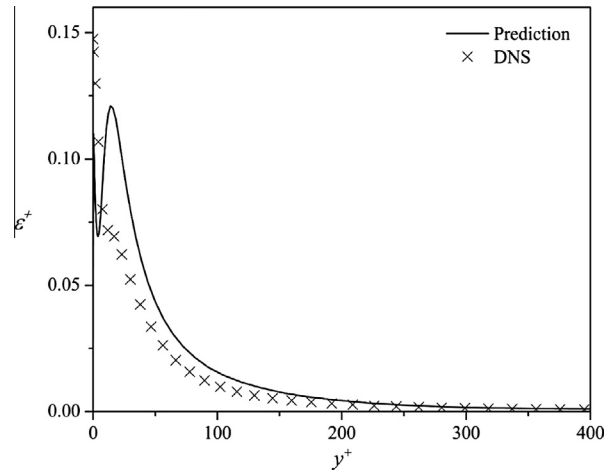**Fig. 12.** Comparison between predicted and DNS data of ε^+, for case B.
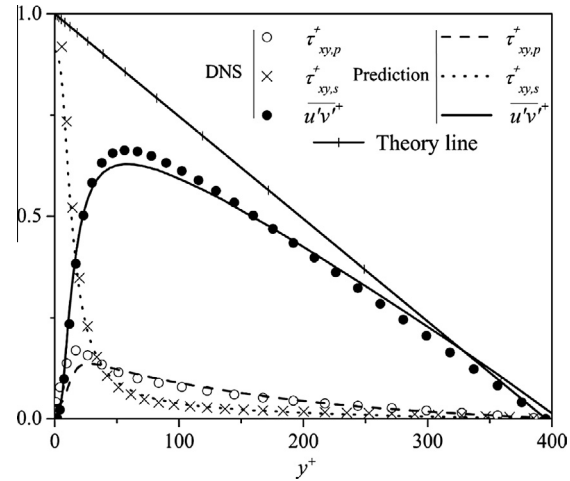

Fig. 13. Comparison between predictions (lines) and DNS data (symbols) of normalized shear stresses for case B.

B ($DR = 37\%$, Table 1). Fig. 8 compares its predictions and performance against DNS data. The model developed by Iaccarino et al. [24] relates NLT_{kk} with ε, which according to Fig. 1, on account of the location of the peak in ε and its behavior far from the wall is less accurate compared with DNS. As a result of the developed closures for M_{kk}, and NLT_{kk} the trace of the polymer stress (τ_{kk}) is depicted in Fig. 9, which is calculated from Eq. (30) while neglecting CT_{kk}.

The proposed closure for NLT_{kk} is always positive, whereas the DNS data of Fig. 8 shows a small incursion of NLT_{kk} into negative values near the wall. However, Fig 6(a) and (b) also shows these negative peaks in NLT_{kk} to be negligible as compared with M_{kk}, which is nearly 100 times bigger than NLT_{kk} close to the wall, so that neglecting the negative peak of NLT_{kk} is of no consequence to the predictions of C_{kk}, as seen in Fig. 9, and in addition it prevents possible numerical divergence.

3.2. Development of closures needed by k, ε, and $\overline{v^2}$ equations

Closures are required for two terms in the transport equation of k, namely for the viscoelastic turbulent transport (Q_p) and the viscoelastic stress work (ε_p). Similarly, the corresponding terms need to be modeled in the transport equation of $\overline{v^2}$, namely the transverse viscoelastic turbulent transport ($Q_{yy,p}$) and the transverse viscoelastic stress work ($\varepsilon_{yy,p}$). Finally, it is also necessary to provide a

Fig. 11. Comparison between predicted and DNS data of k^+ and $\overline{v^2}$ for case B.

closure for the term accounting for the viscoelastic contribution to the transport equation of ε denoted by E_p. Figs. 1 and (2) showed the budgets of k and $\overline{v^2}$ obtained from DNS data, respectively. In both cases the viscoelastic turbulent transport is negligible as also found previously [21] and in particular also by the independent DNS data of [24,33].

The viscoelastic stress work (ε_p) appearing in the transport equation of k is defined as

$$\varepsilon_p = \frac{1}{\rho}\overline{\tau_{ij}^p\frac{\partial u_i}{\partial x_j}}$$
$$= \frac{\eta_p}{\rho\lambda}\left[\overline{C_{ij}f(C_{mm}+c_{mm})\frac{\partial u_i}{\partial x_j}} + \overline{c_{ij}f(C_{mm}+c_{mm})\frac{\partial u_i}{\partial x_j}}\right] \quad (34)$$

Pinho et al. [21,23] showed that in low drag reduction the triple correlation can be decoupled into a product of function $f(C_{kk})$ by the remaining double correlation, which is $NLT_{kk}/2$, therefore they approximated the viscoelastic stress work by

$$\varepsilon_p \approx \frac{\eta_p}{2\rho\lambda}f(C_{mm})\left[\overline{c_{ij}\frac{\partial u_i}{\partial x_j}}\right] = \frac{\eta_p}{2\rho\lambda}f(C_{mm})NLT_{kk} \quad (35)$$

Fig. 10 shows that this closure remains valid for intermediate and high drag reductions without the need for the coefficient of 1.076 introduced in [21].

By contrast Iaccarino et al. [24] modeled the viscoelastic stress work by

$$\varepsilon_p = b\lambda kS^2 \quad (36)$$

where b is a constant, λ is the polymer relaxation time, k is the turbulent kinetic energy, and S represents the magnitude of the strain rate. Fig. 10 compares performance of both closures with DNS data for intermediate and high drag reduction. Clearly the model of Iaccarino et al. [24] excessively dampens ε_p far from the wall, whereas the current model (Eq. (35)) is a better representation of DNS data all across the channel.The other term that needs closure is the transverse component of the viscoelastic stress work $\varepsilon_{yy,p}$. Fig. 2 shows the budgets of different terms in $\overline{v^2}$ equation. For Newtonian fluids, Lien and Durbin [31] modeled the transverse component of the velocity–pressure gradient term by the source term (kf) in the $\overline{v^2}$ transport equation. The true closure for $\varepsilon_{yy,p}$ must be a function of NLT_{yy} as presented in Eq. (34), however due to the fact that in this work we only considered the trace of the time averaged constitutive equation in the following an alternative approach is introduced. The DNS data plotted in Fig. 2 include the source term (kf) and the transverse component of the viscoelastic stress work for LDR and HDR. Regardless of the amount of drag reduction the transverse component of the polymer stress work follows nearly the same trends as the source term (kf), which suggests that the largest positive quantity in the $\overline{v^2}$ transport equation, i.e. the pressure strain term (here kf), is the main responsible for accounting for the energy absorbed by the polymers. Therefore, to close the transverse component of the viscoelastic stress work the source term (kf) in the $\overline{v^2}$ transport equation was used together with the turbulent viscoelastic Prandtl number ($Pr_{T,p}$) as:

$$\varepsilon_{p,yy} = a_3\sqrt{Wi_{\tau 0}}Pr_{T,p}kf \quad (37)$$

The last term in Eq. (22) (Φ_{22}^p) represents the viscoelastic contribution to the f equation. Leighton et al. [20] introduced an explicit modification to the pressure–strain correlation to account for the polymer-induced turbulence energy redistribution, but Iaccarino et al. [24] tested this formulation and found that it did not produce acceptable results for high drag reduction. Similarly, we tested this term and found that by using it there is an excessive damping of the wall normal fluctuations leading to a complete flow laminarization. Therefore, this term was neglected as was also previously the case

in [24]. Fig. 11 compares DNS and predicted k and $\overline{v^2}$ by using the above developed closures, all across the channel.

The last quantity that needs to be modeled is the viscoelastic contribution to the transport equation of ε, denoted as E_p. A closure was developed by Resende et al. [23], but here we adopt a much simpler approach. E_p is assumed to be a destruction term [23] and to devise its closure we followed the same approach as for the classical Newtonian destruction term in the ε equation, but involving a viscoelastic quantity, i.e., we assumed that this rate is proportional to the ratio of the viscoelastic stress work (usually acting as a viscoelastic dissipation of k, cf. Fig. 1) and the time scale $1/T_t$. The viscoelastic destruction term is therefore modeled as equation (38).

$$E_p = \frac{C_{\varepsilon 1}\varepsilon_p}{T_t} \quad (38)$$

Consequently the solvent dissipation rate transport equation is closed as

$$U_j\frac{\partial\varepsilon}{\partial x_j} = \frac{C_{\varepsilon 1}(P_k - \varepsilon_p) - C_{\varepsilon 2}\varepsilon}{T_t} + \frac{\partial}{\partial x_j}\left(\left(v + \frac{v_T}{\sigma_\varepsilon}\right)\frac{\partial\varepsilon}{\partial x_j}\right) \quad (39)$$

Fig. 12 shows the performance of the model in predicting the dissipation rate.

We next compare in Fig. 13 the overall shear stress balance for case B (Table 1), as predicted by this model, with the corresponding DNS balance. It includes the Reynolds stress, the solvent stress, and the polymer stress.
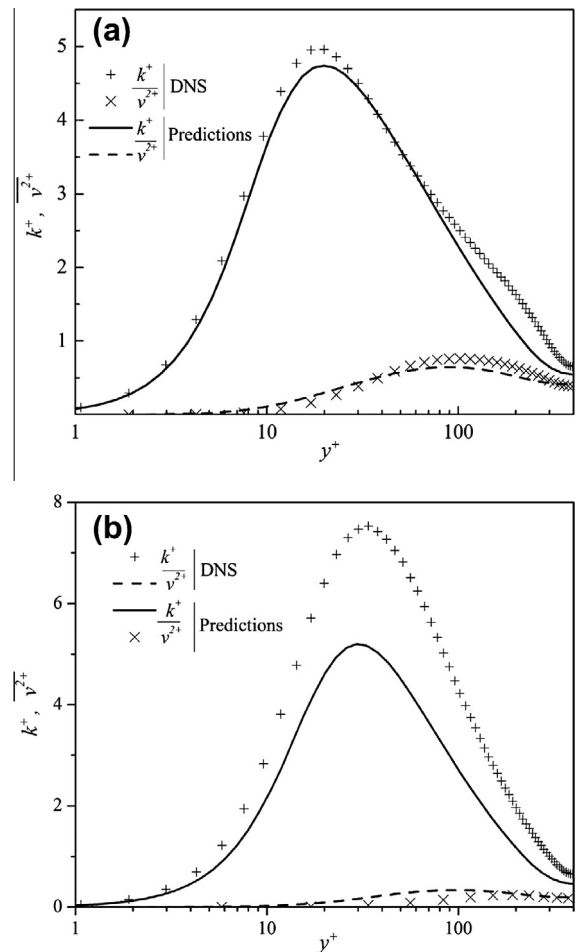

Fig. 14. Turbulent kinetic energy and $\overline{v^2}$, (a) case A (LDR), and (b) case D (HDR).
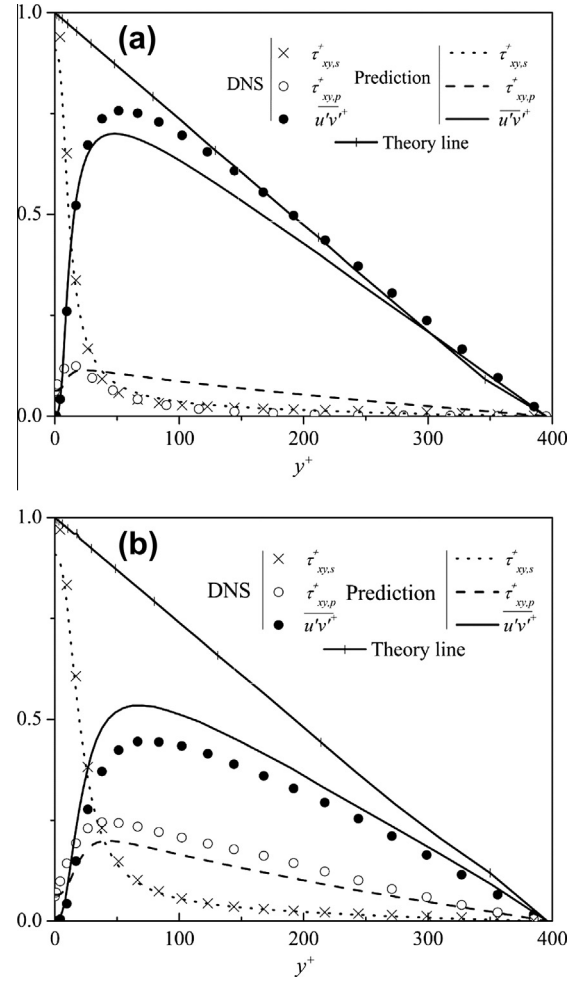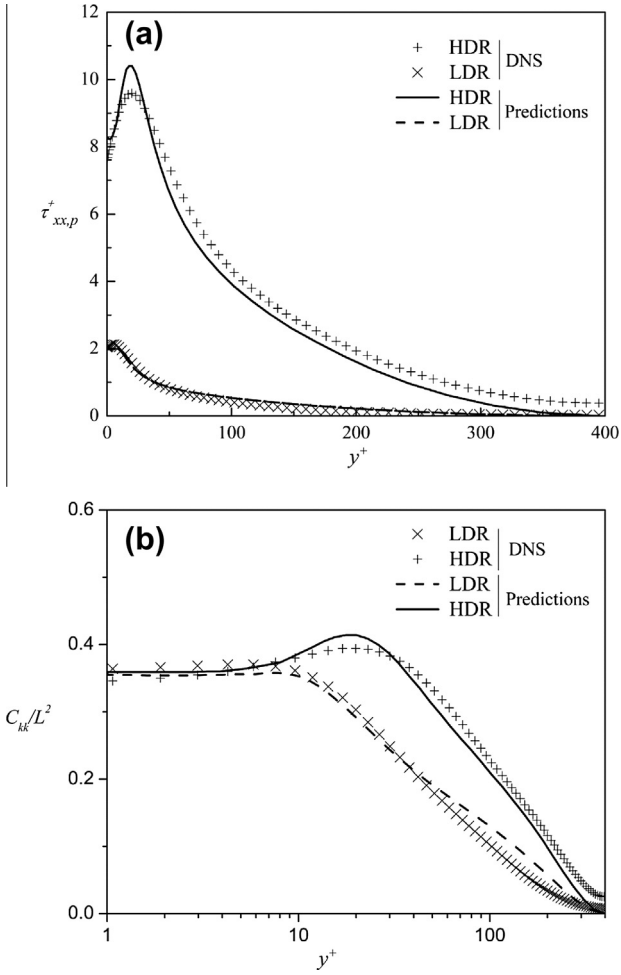
Fig. 15. Comparison between predictions (lines) and DNS data (symbols) for (a) Polymer stress, and (b) polymer length normalized by polymer maximum length, at $Re_{\tau 0} = 395$.

Fig. 16. Comparison between predictions (lines) and DNS data (symbols) for normalized shear stresses (a) case A (LDR), and (b) case D (HDR).

3.3. Summary of the model (See footnote in page 5)

Utilizing the closures developed in the previous subsections, the governing and model equations are given below.

$$\rho \frac{\partial U_i}{\partial t} + \rho U_k \frac{\partial U_i}{\partial x_k} = -\frac{\partial \overline{P}}{\partial x_i} + \rho \frac{\partial}{\partial x_k}\left[(v_s + v_T + v_{T,p})\frac{\partial U_i}{\partial x_k}\right] \tag{40}$$

$$U_j \frac{\partial k}{\partial x_j} = P_k - \varepsilon + \frac{\partial}{\partial x_j}\left(\left(v_s + \frac{v_T}{\sigma_k}\right)\frac{\partial k}{\partial x_j}\right) - \varepsilon_p \tag{41}$$

$$U_j \frac{\partial \varepsilon}{\partial x_j} = \frac{C_{\varepsilon 1}P_k - C_{\varepsilon 2}\varepsilon}{T_t} + \frac{\partial}{\partial x_j}\left(\left(v_s + \frac{v_T}{\sigma_\varepsilon}\right)\frac{\partial \varepsilon}{\partial x_j}\right) - E_p \tag{42}$$

$$U_j \frac{\partial \overline{v^2}}{\partial x_j} = kf + \frac{\partial}{\partial x_j}\left(\left(v_s + \frac{v_T}{\sigma_k}\right)\frac{\partial \overline{v^2}}{\partial x_j}\right) - 6\frac{\varepsilon}{k}\overline{v^2} - \varepsilon_{p,yy} \tag{43}$$

$$f - L_t^2 \frac{\partial^2 f}{\partial x_j \partial x_j} = C_1 \frac{\left(\frac{2}{3} - \frac{\overline{v^2}}{k}\right)}{T_t} + C_2 \frac{P_k}{k} - 5\varepsilon\frac{\overline{v^2}}{k} \tag{44}$$

$$M_{kk} + NLT_{kk} + \frac{1}{\lambda}(3 - f(C_{kk})C_{kk}) = 0 \tag{45}$$

where

$$v_{T,p} = \left(\frac{v_p}{f(C_{kk})} + a_1\sqrt{L^2/Wi_{\tau o}}f(C_{kk})\,v_T\right) \tag{46}$$
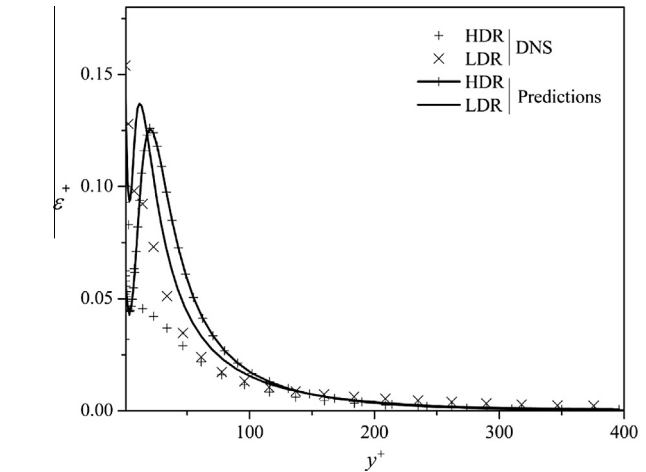

Fig. 17. Comparison between predictions and DNS data of ε^+ for case A (LDR), and case D (HDR).

$$M_{kk} = 2\left\{\frac{\lambda}{f(C_{kk})}\frac{v_{T,p}}{v_p}\left(\frac{dU}{dy}\right)^2\right\} \tag{47}$$

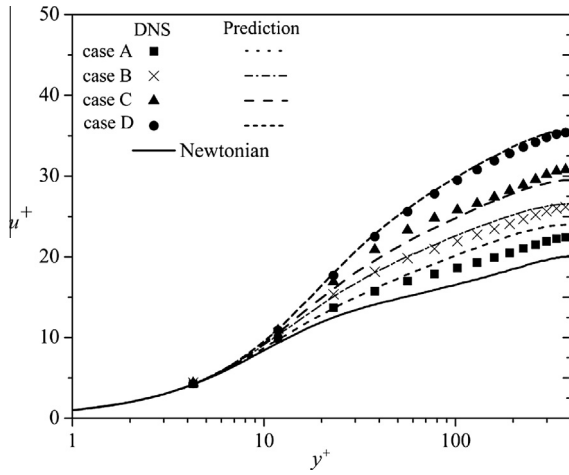$$NLT_{kk} = a_2 M_{kk}\frac{v_T}{v_o} \tag{48}$$

Fig. 18. Normalized velocity profiles in wall coordinates for Newtonian and FENE-P fluids with rheological parameters defined in Table 1, at $Re_{\tau 0} = 395$.
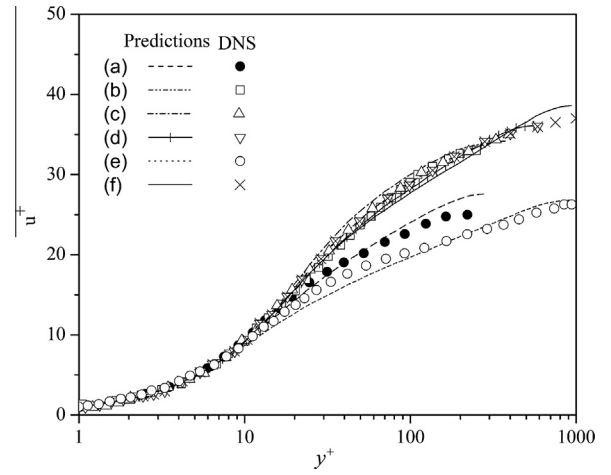

Fig. 20. Comparison between predictions and independent DNS data of the normalized velocity profiles in wall coordinates for turbulent FENE-P flows with flow conditions defined in Table 2.
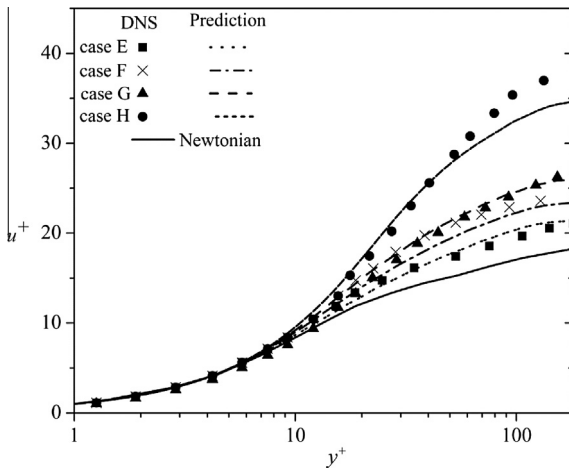
Table 2
Independent DNS data.

DNS data	Case	$Re_{\tau 0}$	L^2	$Wi_{\tau 0}$
Iaccarino et al. [24]	(a)	300	10,000	36
Iaccarino et al. [24]	(b)	300	10,000	120
Thais et al. [36]	(c)	395	10,000	116
Thais et al. [36]	(d)	590	10,000	116
Thais et al. [33]	(e)	1000	900	50
Thais et al. [33]	(f)	1000	10,000	115

Fig. 19. Normalized velocity profiles in wall coordinates for Newtonian and FENE-P flows with rheological parameters defined in Table 1, at $Re_{\tau 0} = 180$.

$$\varepsilon_p = \frac{\eta_p}{2\rho\lambda} f(C_{mm}) NLT_{kk} \qquad (49)$$

$$\varepsilon_{p,yy} = a_3 \sqrt{Wi_{\tau 0}} Pr_{T,p} kf \qquad (50)$$

$$E_p = \frac{C_{\varepsilon 1}\varepsilon_p}{T_t} \qquad (51)$$

Relative to the model of Lien and Durbin [31] this model has 3 extra coefficients to incorporate the polymer effects, $a_1 = 0.02$, $a_2 = 0.16$ and $a_3 = 0.15$. Other coefficients arise from the Newtonian model and take the same numerical values as reported in [31], the coefficient C_μ also exists in the context of Newtonian fluid models, but here it was modified to take the numerical value of 0.16 instead of the original value of 0.19. The boundary conditions are those of no slip for velocities, k and $\overline{v^2}$, whereas for the dissipation by the solvent and f we used the standard conditions of Newtonian fluids described in [31].

4. Results and discussion

In this section, results from several predictions of fully-developed channel flow using this model are presented and assessed against other sets of DNS data for FENE-P fluids as in Table 1. All

viscoelastic flow calculations were carried out using the same channel dimensions and friction velocity as for the DNS. Note that some comparisons involve DNS data for $Re_{\tau 0} = 180$, and also the independent DNS results of [24,33,36].

The predicted k and $\overline{v^2}$ profiles are shown in Fig. 14 for cases A and D. It is well known [30,34,35] that streamwise velocity fluctuations $\overline{u^2}$ increase with DR, while the wall normal and spanwise components $\overline{v^2}$ and $\overline{w^2}$ monotonically decrease. The increase of $\overline{u^2}$ is larger than the decrease of $\overline{v^2}$ and $\overline{w^2}$ and as a consequence the turbulent kinetic energy slightly increases. Moreover the peak location of k shifts away from the wall as DR increases, which is consistent with the upward shift of the logarithmic region in the mean velocity profile. As it is shown in Fig. 14 the predictions have a satisfactory agreement with DNS data and the model captures both the physical characteristics of turbulent channel flow of dilute polymer solutions in terms of the slight increase in k and the upward shift of its peak location by increasing DR, as reported in the DNS results and in the experimental findings of Ptasinski et al. [12]. Nevertheless, at HDR (case D in Fig. 14) the model under-predicts the peak value of k^+. As is well known from experiments [12], DR is associated with a decoupling between the streamwise and transverse turbulence accompanied by a reduction in $\overline{v^2}$ and this causes a decrease in the Reynolds shear stress, whereas the streamwise turbulence may even increase slightly before a decrease at very high DR. In the model the reduction in $\overline{uv}$ is accomplished by the eddy viscosity and by adopting Durbin's model of Eq. (16) and this reduction can be achieved via a decrease in turbulent time scale and/or wall normal Reynolds stress. The reduction in $\overline{v^2}$ is accurately predicted for all cases, but is insufficient to reduce $\overline{uv}$ as much as needed at HDR, so the turbulent time scale must also decrease and this can be achieved via a decrease in k and/or an increase in ε. However, since ε is also reduced (cf. Fig. 1a and b), there is still the need for a reduction in k at HDR and this explains the discrepancy. One remedy in the context of
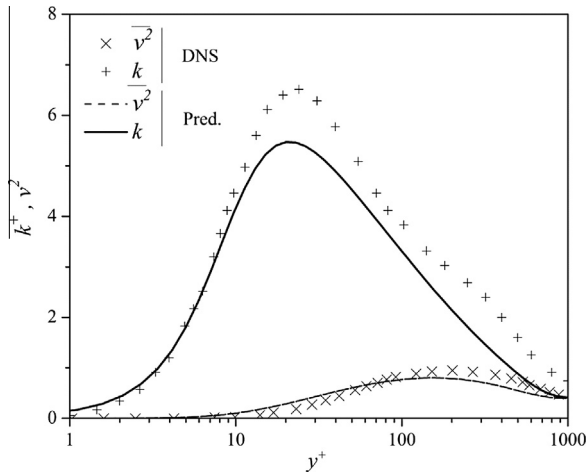
Fig. 21. Comparison between predictions and DNS for the transverse profiles of k^+ and $\overline{v^2}$ for $Re_{\tau 0} = 1000$, $We_{\tau 0} = 50$, and $L^2 = 900$ (case (e) in Table 2).
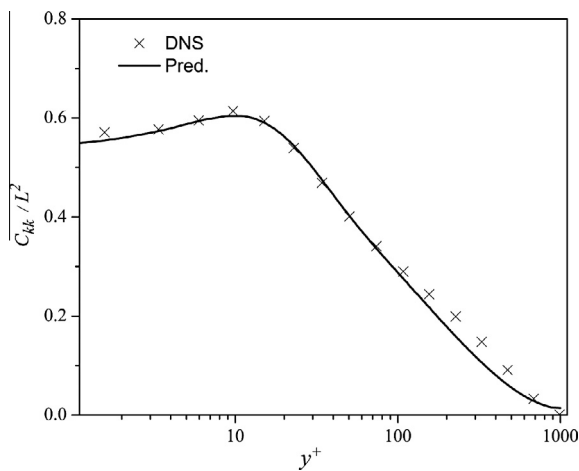

Fig. 22. Comparison between predictions and DNS for the polymer length normalized by polymer maximum length for $Re_{\tau 0} = 1000$, $We_{\tau 0} = 50$, and $L^2 = 900$ (case (e) in Table 2).

this model could be the use of a damping function for the eddy viscosity, which we decided not to do in order to maintain the original idea of Durbin's theory (the elimination of damping functions). The other remedy can be the use of a higher level turbulence model, but this is beyond the scope of this work.

We should add that this problem is here limited to HDR and is much more alleviated than with two equation models that do not rely on $\overline{v^2}$, as discussed in Resende et al. [23] where a severe reduction in k was observed already at intermediate DR even when using damping functions.

Finally, we should also mention that the discrepancy may be somewhat fictitious: in the experiments of Ptasinski et al. [12] the stream wise turbulence ($\overline{u^2}$) increases slightly by increasing DR with a peak of u_{rms} reaching around 3.2 corresponding to a peak for k of around 5.5. On the other hand their corresponding DNS results over-predict those peak values (maximum u_{rms} of around 4.5, and maximum k of around 8.5). They extensively discuss this difference and state that this might be due to shortcomings in the FENE-P model.

Predictions of the trace of the polymer stress and of the conformation tensor are compared with DNS data in Fig. 15(a) and (b), respectively for case A (LDR) and D (HDR). Note that the region of high chain dumbbell extension is limited to the near wall region ($y^+ < 50$), which is in agreement with findings of [28].

In a fully developed state, the total shear stress must follow a straight line across the channel varying from zero at the centerline to the wall shear stress (τ_w) at the wall. Here the total shear stress is the sum of three contributions, namely, the Reynolds stress, the viscous stress of the solvent and the polymer stress. The total shear stress profile and its three components are plotted in Fig. 16 normalized by the wall shear stress for low and high drag reduction (cases A and D) and compared with the corresponding DNS. In both cases the total shear stress follows the expected linear profiles over the channel height, indicating that a stationary fully developed state has been reached. In low drag reduction case the polymer stress contribution is relatively small, and it occurs mainly in the near wall region. However, as DR increases, the Reynolds stress is significantly reduced, and correspondingly the polymer stress increases to ensure the balance and becomes comparable to the Reynolds stress. Specifically, at HDR the Reynolds stress is significantly reduced as compared to the LDR regime, but it remains non-zero. In the LDR case the proposed model predicts the peak and the general trend of all stresses very well. In HDR case the polymer contribution becomes important and clearly the prediction of the proposed closure is good. These observations are consistent with the numerical findings of [28] and the experimental results of Ptasinski et al. [12].

In Fig. 17 the predictions of the dissipation rate are compared with the DNS data for both LDR (case A) and HDR (case D). At LDR the predictions are accurate near and far from the wall, while at HDR the predictions are accurate far from the wall, but overpredicted close to the wall.

We present predicted transverse profiles of the mean streamwise velocity for a large set of data covering the whole range of DR, different values of L^2, Reynolds numbers, and Weissenberg numbers in Figs. 18–20, and comparing the profiles with the corresponding DNS data. For the sake of comparison the profiles for Newtonian flow at each Reynolds number have also been included. All profiles in the viscous sublayer collapse on the linear distribution $U^+ = y^+$. Further away from the wall the mean velocity of the drag reduced flows increases as compared to that in Newtonian flows. Specifically in the LDR regime, the logarithmic profile is shifted upwards but remains parallel to that of the Newtonian flow as is also found in the DNS results. The upward shift of the logarithmic profile can be interpreted as a thickening of the buffer layer. In the HDR regime, the slope of the mean velocity has augmented as the thickened buffer layer occupies nearly the whole channel. In addition, the slope increases as a function of DR and the predictions and DNS are consistent and this is seen to be the case at both high and low Reynolds numbers in Figs. 18 and 19.

We also assessed the model performance in predicting drag reduction against independent DNS data provided by [24,33,36], which corresponds to $Re_{\tau 0}$ = 300, 395, 590, 1000, i.e., including high Reynolds number flows. As seen in Fig. 20, the agreement between the predictions and the DNS profiles of the mean velocity for the cases in Table 2 is fairly good regardless of the Reynolds number. The comparisons between the DNS data and the predictions in terms of k, $\overline{v^2}$, and C_{kk} for the high Reynolds number flow case (e) ($Re_\tau = 1000$) are presented in Figs. 21 and 22 and show again a good agreement, similar to that observed at lower Reynolds number flows.

5. Conclusions

The $k - \varepsilon - \overline{v^2} - f$ model of Lien and Durbin [31] is modified for modeling turbulent channel flow of dilute polymer solutions up to the maximum drag reduction. Fluid rheology is described by the finitely extensible nonlinear elastic-Peterlin (FENE-P) constitutive equation and to help develop the model eight sets of recent direct

numerical simulations (DNS) data are analyzed. To account for the polymer shear stress term in the Reynolds averaged momentum equation the procedure proposed by Iaccarino et al. [24] is used and a turbulent viscoelastic viscosity is introduced in order to calculate the polymer shear stress via a Boussinesq-like relationship which is consistent with current DNS and independent DNS simulations.

Analysis of the DNS results confirms the previously developed closure [21] for the viscoelastic stress work on the basis of NLT_{kk}, which is a new contribution to the transport equation of k, but now with a unit coefficient. A simple closure for NLT_{kk} is proposed by using M_{kk} and the turbulent eddy viscosity. A closure was also proposed for the transverse polymer stress work in the $\overline{v^2}$ transport equation leading to a modification of the original Newtonian source term developed by Lien and Durbin [31] to account for the reduction of the pressure-strain redistribution term. The f equation remained the same as for Newtonian fluids. Finally, the closure for the viscoelastic destruction of the rate of dissipation by the solvent has similarities with the classical Newtonian destruction term.

All closures were developed on the basis of DNS data for 37% drag reduction at $Re_{\tau 0} = 395$ and the performance assessed against sets of DNS data for a wide range of Reynolds numbers ($Re_{\tau 0} = 180$, 300, 395, 590 and 1000) over a wide range of Weissenberg numbers together with different values of L^2 and β and also against independent DNS results.

The predictions in fully-developed channel flow compare very well with DNS data in terms of mean velocity, turbulent kinetic energy and viscoelastic stresses at all ranges of drag reduction. The turbulence model here developed does not require wall damping functions as the original model of Lien and Durbin [31] and the new closures required to account for viscoelastic fluid behavior are simple and numerically inexpensive with the model showing effectively a better predictive capability than existing models for FENE-P fluids.

Acknowledgements

References

[1] J.W. Hoyt, The effect of additives on fluid friction, ASME J. Basic Eng. 94 (1972) 258–285.
[2] J.L. Lumley, Drag reduction by additives, Annu. Rev. Fluid Mech. 1 (1969) 367–384.
[3] J.L. Lumley, Drag reduction in turbulent flow by polymer additives, J. Poly. Sci. 7 (1973) 263–290.
[4] P.S. Virk, Drag reduction fundamentals, AIChE J. 21 (1975) 625–656.
[5] P.S. Virk, An elastic sublayer model for drag reduction by dilute solutions of linear macromolecules, J. Fluid Mech. 45 (1971) 417–440.
[6] W. Castro, W. Squire, The effect of polymer additives on transition in pipe flow, Appl. Sci. Res. 18 (1967) 81–96.
[7] W.B. Giles, W.T. Pettit, Stability of dilute viscoelastic flows, Nature 216 (11) (1967) 470–472.
[8] M. Tabor, P.G. De Gennes, A cascade theory of drag reduction, Europhys. Lett. 2 (1986) 519–522.

[9] L. Xi, M.D. Graham, Active and hibernating turbulence in minimal channel flow of Newtonian and Polymeric fluids, Phys. Rev. Lett. 104 (2010) 218301.
[10] R. Sureshkumar, A.N. Beris, R.A. Handler, Direct numerical simulation of the turbulent channel flow of a polymer solution, Phys. Fluids 9 (1997) 743–755.
[11] Y. Dubief, C.M. White, V.E. Terrapon, E.S.G. Shaqfeh, P. Moin, S.K. Lele, On the coherent drag reducing and turbulence enhancing behavior of polymers in wall flows, J. Fluid Mech. 514 (2004) 271–280.
[12] P.K. Ptasinski, B.J. Boersma, F.T.M. Nieuwstadt, M.A. Hulsen, B.H.A.H. van den Brule, J.C.R. Hunt, Turbulent channel flow near maximum drag reduction: simulations, experiments and mechanisms, J. Fluid Mech. 490 (2003) 251–291.
[13] K. Kim, C.F. Li, R. Sureshkumar, S. Balachandar, R.J. Adrian, Dynamics of hairpin vortices and polymer-induced turbulent drag reduction, Phys. Rev. Lett. 100 (2008) 134504.
[14] K. Kim, C.F. Li, R. Sureshkumar, S. Balachandar, R.J. Adrian, Effects of polymer stresses on eddy structures in drag-reduced turbulent channel flow, J. Fluid Mech. 584 (2007) 281–300.
[15] C.D. Dimitropoulos, Y. Dubief, E.S.G. Shaqfeh, P. Moin, S.K. Lele, Direct numerical simulation of polymer-induced drag reduction in turbulent boundary layer flow, Phys. Fluids 17 (2005) 011705.
[16] C.F. Li, R. Sureshkumar, B. Khomami, Influence of rheological parameters on polymer induced turbulent drag reduction, J. Non-Newton. Fluid Mech. 140 (2006) 23–40.
[17] F.T. Pinho, A GNF framework for turbulent flow models of drag reducing fluids and proposal for a k–ε type closure, J. Non-Newton. Fluid Mech. 114 (2003) 149–184.
[18] P.R. Resende, M.P. Escudier, F. Presti, F.T. Pinho, D.O.A. Cruz, Numerical predictions and measurements of Reynolds normal stresses in turbulent pipe flow of polymers, Int. J. Heat Fluid Flow 27 (2006) 204–219.
[19] P.R. Resende, F.T. Pinho, D.O.A. Cruz, A Reynolds stress model for turbulent flows of viscoelastic fluids. J. Turbul. 2013. (accepted for publication)
[20] R.I. Leighton, D.T. Walker, T.R. Stephens, G.C. Garwood, Reynolds-stress modeling for drag-reducing viscoelastic flow, in: 2003 Joint ASME/JSME Fluids Engineering Symposium on Friction Drag Reduction, Honolulu, Hawaii, USA, 2003.
[21] F.T. Pinho, C.F. Li, B.A. Younis, R. Sureshkumar, A low Reynolds number k–ε turbulence model for FENE-P viscoelastic fluids, J. Non-Newton. Fluid Mech. 154 (2008) 89–108.
[22] F.T. Pinho, C.F. Li, B.A. Younis, R. Sureshkumar, Corrigendum to "A low Reynolds number turbulence closure for viscoelastic fluids", J. Non-Newton. Fluid Mech. 51 (2012) 181–182.
[23] P.R. Resende, K. Kim, B.A. Younis, R. Sureshkumar, F.T. Pinho, A FENE-P k–ε turbulence model for low and intermediate regimes of polymer-induced drag reduction, J. Non-Newton. Fluid Mech. 166 (2011) 639–660.
[24] G. Iaccarino, E.S.G. Shaqfeh, Y. Dubief, Reynolds-averaged modeling of polymer drag reduction in turbulent flows, J. Non-Newton. Fluid Mech. 165 (2010) 376–384.
[25] C.D. Dimitropoulos, R. Sureshkumar, A.N. Beris, R.A. Handler, Budgets of Reynolds stress, kinetic energy and streamwise enstrophy in viscoelastic turbulent channel flow, Phys. Fluids 13 (4) (2001) 1016–1027.
[26] R.B. Bird, P.J. Dotson, N.L. Johnson, Polymer solution rheology based on a finitely extensible bead-spring chain model, J. Non-Newton. Fluid Mech. 7 (1980) 213–235.
[27] R.B. Bird, C.F. Curtiss, R.C. Armstrong, O. Hassager, Dynamics of Polymeric Liquids Kinetic Theory, 2nd ed., vol. 2, John Wiley & Sons, New York, 1987.
[28] C.F. Li, V.K. Gupta, R. Sureshkumar, B. Khomami, Turbulent channel flow of dilute polymeric solutions: drag reduction scaling and an eddy viscosity model, J. Non-Newton. Fluid Mech. 139 (2006) 177–189.
[29] A.N. Beris, B.J. Edwards, Thermodynamics of Flowing Systems with Internal Microstructure, Oxford University Press, New York, 1994.
[30] K.D. Housiadas, A.N. Beris, R.A. Handler, Viscoelastic effects on higher order statistics and coherent structures in turbulent channel flow, Phys. Fluids 17 (2005) 35106.
[31] F.S. Lien, P.A. Durbin, Non linear $\kappa - \varepsilon - \overline{v^2} - f$ modelling with application to high-lift, in: Proceedings of the Summer Program 1996, Stanford University, 1996, pp. 5–22.
[32] P.A. Durbin, Near-wall turbulence closure modeling without damping functions, Theor. Comp. Fluid Dyn. 3 (1991) 1–13.
[33] L. Thais, T.B. Gatski, G. Mompean, Analysis of polymer drag reduction mechanisms from energy budgets, Int. J. Heat Fluid Flow (2013), http://dx.doi.org/10.1016/j.ijheatfluidflow.2013.05.016.
[34] D.K. Oldaker, W.G. Tiederman, Spatial structure of the viscous sublayer in drag-reducing channel flows, Phys. Fluids 20 (1977) S133–S144.
[35] W.G. Tiederman, T.S. Luchik, D.G. Boggard, Wall-layer structure and drag reduction, J. Fluid Mech. 156 (1985) 419–437.
[36] L. Thais, T.B. Gatski, G. Mompean, Some dynamical features of the turbulent flow of a viscoelastic fluid for reduced drag, J. Turbul. 13 (2012) 1–26.